EBioMedicine 48 (2019) 425–441

Contents lists available at ScienceDirect

EBioMedicine

journal homepage: www.ebiomedicine.com

EBioMedicine
Published by THE LANCET

Research paper

High levels of serum hyaluronan is an early predictor of dengue warning signs and perturbs vascular integrity

Chun-Yu Lin [a,b,c,f], Constantinos Kolliopoulos [a], Chung-Hao Huang [b,c], Jyrki Tenhunen [f,g], Carl-Henrik Heldin [a], Yen-Hsu Chen [c,d,e,*,1], Paraskevi Heldin [a,**,1]

[a] Department of Medical Biochemistry and Microbiology, Uppsala University, Box 582, SE-751 23 Uppsala, Sweden
[b] Division of Infectious Diseases, Department of Internal Medicine, Infection Control Center, Kaohsiung Medical University Hospital, Kaohsiung Medical University, Kaohsiung 807, Taiwan
[c] School of Medicine, Graduate Institute of Medicine, Sepsis Research Center, Center of Dengue Fever Control and Research, Kaohsiung Medical University, Kaohsiung, Taiwan
[d] Deparent of Internal Medicine, Kaohsiung Municipal Ta-Tung Hospital, Kaohsiung, Taiwan
[e] Department of Biological Science and Technology, College of Biological Science and Technology, National Chiao Tung University, HsinChu, Taiwan
[f] Department of Surgical Sciences, Uppsala University, Akademiska Hospital, 751 85 Uppsala, Sweden
[g] Critical Care Medicine Research Group, Department of Intensive Care, Tampere University Hospital, Tampere, Finland

ARTICLE INFO

Article history:
Received 10 May 2019
Received in revised form 30 August 2019
Accepted 6 September 2019
Available online 13 September 2019

Keywords:
CD44
Dengue
Hyaluronan
Vascular leakage
VE-cadherin
Cytokines
HAS2
HYAL2
TGFbeta

ABSTRACT

Background: A main pathological feature of severe dengue virus infection is endothelial hyper-permeability. The dengue virus nonstructural protein 1 (NS1) has been implicated in the vascular leakage that characterizes severe dengue virus infection, however, the molecular mechanisms involved are not known.
Methods: A cohort of 250 dengue patients has been followed from the onset of symptoms to the recovery phase. Serum hyaluronan levels and several other clinical parameters were recorded. The effect of NS1 treatment of cultured fibroblasts and endothelial cells on the expressions of hyaluronan synthetic and catabolic enzymes and the hyaluronan receptor CD44, were determined, as have the effects on the formation of hyaluronan-rich matrices and endothelial permeability.
Findings: Elevated serum hyaluronan levels (≥70 ng/ml) during early infection was found to be an independent predictor for occurrence of warning signs, and thus severe dengue fever. High circulating levels of the viral protein NS1, indicative of disease severity, correlated with high concentrations of serum hyaluronan. NS1 exposure decreased the expression of CD44 in differentiating endothelial cells impairing the integrity of vessel-like structures, and promoted the synthesis of hyaluronan in dermal fibroblasts and endothelial cells in synergy with dengue-induced pro-inflammatory mediators. Deposited hyaluronan-rich matrices around cells cultured in vitro recruited CD44-expressing macrophage-like cells, suggesting a mechanism for enhancement of inflammation. In cultured endothelial cells, perturbed hyaluronan-CD44 interactions enhanced endothelial permeability through modulation of VE-cadherin and cytoskeleton re-organization, and exacerbated the NS1-induced disruption of endothelial integrity.
Interpretation: Pharmacological targeting of hyaluronan biosynthesis and/or its CD44-mediated signaling may limit the life-threatening vascular leakiness during moderate-to-severe dengue virus infection.
Fund: This work was supported in part by grants from the Swedish Cancer Society (2018/337; 2016/445), the Swedish Research Council (2015-02757), the Ludwig Institute for Cancer Research, Uppsala University, the Ministry of Science and Technology, Taiwan (106–2314-B-037-088- and 106–2915-I-037-501-), Kaohsiung Medical University Hospital (KMUH103-3 T05) and Academy of Finland. The funders played no role in the design, interpretation or writing of the manuscript.

1. Introduction

The glycosaminoglycan hyaluronan is present in virtually all tissues in the body, and plays key roles in regulation of tissue homeostasis, including vascular integrity [1–4]. An aberrant accumulation of hyaluronan occurs in inflammation/infection and cancer, conditions where a plethora of growth factors, cytokines and chemokines are

Abbreviations: HAS, Hyaluronan synthase; HYAL, hyaluronidase; LYVE1, Lymphatic Vessel Endothelial Hyaluronan Receptor 1; RHAMM, receptor for hyaluronan mediated motility; TMEM2, transmembrane 2.

* Correspondence to: Y-H Chen, Department of Internal Medicine, Kaohsiung Municipal Ta-Tung Hospital, No.68, Jhonghua 3rd Rd, Kaohsiung City 80145, Taiwan.
** Correspondence to: P. Heldin, Uppsala University, Department of Medical Biochemistry and Microbiology, Biomedical Center, Box 582, SE-751 23 Uppsala, Sweden.
E-mail addresses: infchen@gmail.com (Y.-H. Chen), evi.heldin@imbim.uu.se (P. Heldin).
[1] Equal contribution. To whom correspondence should addressed:

https://doi.org/10.1016/j.ebiom.2019.09.014

Research in context

Evidence before this study

Dengue virus infection, transmitted by mosquitos, rapidly increases due to global climate warming and international travelling, and causes suffering and consumes health care resources. A subset of patients, e.g. adults exposed to second infection or being older than 65 years, and infants born by dengue-immune mothers, experience a life-threatening condition including exacerbated inflammation and vascular hyper-permeability. The viral protein NS1 plays a crucial role in these biological outcomes. No suitable animal model exists that recapitulate the human immune-pathological events involved in severe dengue, and there is no effective and safe dengue vaccine. Thus, early biomarkers that can predict severe dengue disease are lacking, and the mechanisms involved in the vascular hyper-permeability have not been elucidated.

Added value of this study

We have studied a large cohort of dengue virus infected patients (Taiwan outbreaks 2014, 2015), and have shown that high circulating NS1 levels, indicative of disease severity, correlate with high concentration of serum hyaluronan. Moreover, hyaluronan levels higher than 70 ng/ml during early infection, was found to be an independent predictor for occurrence of warning signs and thus risk of severe dengue fever. The NS1-induced increase in the levels of polydisperse hyaluronan and its altered organization, together with suppression of its receptor CD44, were found to be accompanied by perturbed endothelial intercellular junctions, including alterations of actin filaments and VE-cadherin and increased paracellular gaps, and enhanced vascular permeability.

Impact

Our findings provide physicians with a useful tool to identify patients at risk and in need of hospitalization. Moreover our findings suggest a mechanism for the increased vascular permeability in severe dengue, and identify hyaluronan-CD44 signaling as a possible target for therapy to alleviate vascular leakage during dengue virus infection.

released [5,6]. Hyaluronan induces signaling through its interactions with cell surface hyaluronan receptors, including CD44 and RHAMM [6–10], resulting in altered cell adhesion, migration and proliferation. The dysregulated synthesis and turnover of hyaluronan in disease is mediated by synthetic (HAS1, HAS2, HAS3) and catabolic (HYAL1,2 and the KIAA1199 homolog TMEM2) enzymes, which are regulated in response to growth factors and cytokines, as well as bacterial and viral infections [5]. The newly synthesized hyaluronan is extruded through the plasma membrane for assembly into pericellular or extracellular matrices [11,12].

Hyaluronan is turned over rapidly by internalization via CD44 expressed by stromal cells and macrophages, and via the hyaluronan receptor LYVE1 in lymphatic endothelial cells [13–16]. The hyaluronan levels in the serum of middle-aged persons is normally 30–40 ng/ml, but increases during certain pathological conditions [15,17]. In inflamed tissues, the amount of hyaluronan increases as a result of altered biosynthesis, degradation and/or capacity for uptake locally and in lymph nodes, liver and kidneys [13], leading to enhanced release of hyaluronan into the general circulation. In blood vessels, some of the hyaluronan is incorporated in the endothelial glycocalyx layer primarily consisting of proteoglycans, glycoproteins and glycosaminoglycans, including hyaluronan which weaves into the glycocalyx interacting with CD44 in caveolae microdomains on the luminal side of the endothelium [1,18,19]. Caveolae microdomains are a special type of lipid rafts where hyaluronan-CD44 signaling takes place affecting actin regulation and contacts between endothelial cells by modulating the expression and distribution of intercellular junction proteins, such as VE-cadherin [1].

In vascular tissues, hyaluronan affects smooth muscle cell proliferation [20,21], endothelial cell differentiation [22–24] and immune cell function [6,25,26]. Thus, hyaluronan has an important role in the regulation of vascular integrity, and its shedding from endothelial glycocalyx correlates to impaired vascular integrity during injury [27,28]. In addition to the glycocalyx layer, the endothelial integrity is controlled by endothelial cell-cell junctions (paracellular pathway) and by vesicular transport structures (transcellular pathway) [29,30].

The rapid spreading of dengue virus infections has become a public health concern, and about 50% of the world's population is now at risk of infection [31]. Dengue is a vector-borne virus that is transmitted to human host by mosquito skin bites. Clinically, dengue infection is characterized by febrile, critical and recovery phases. Moreover, the disease is characterized by vascular leakage and sometimes a severe life-threatening bleeding that has been linked to exacerbated immune cell activation [32–34]. High levels of the dengue nonstructural protein 1 (NS1) in the circulation, induces release of inflammatory cytokines from infected monocytes and T cells via binding to Toll-like receptor 4 (TLR4) receptors, promoting vascular leakage [32,35–38]. NS1 affects the integrity of endothelial cell monolayers by disruption of components in the endothelial glycocalyx layer [36,39]. However, the molecular and immunological mechanisms underlying the role of NS1 in the pathogenesis of severe dengue infection are not well understood [33].

In this study, we report that high serum hyaluronan levels can serve as a biomarker to predict occurrence of warning signs during the course of dengue virus infection, helping clinicians to make a decision whether hospitalization of patients is needed. Moreover, we present a possible mechanism whereby NS1-induced hyaluronan production is involved in vascular leakage.

2. Materials and methods

2.1. Ethics statement and patients´ enrollment

The human study protocol was approved by the Institutional Review Board (IRB) of Kaohsiung Medical University Hospital (IRB Number: KMUH-IRB-20110451). Informed consent was obtained from all subjects. There were outbreaks of dengue in Taiwan August 2014 to January 2015, and August 2015 to January 2016 [40,41]. Patients (≥20 years) were prospectively enrolled, and their blood samples were provided on the first day of hospital visit, as well as three and seven days later, if the patient was still in the hospital and agreed to provide more samples. The time of symptoms onset for each patient was recorded immediately after enrollment to minimize recalling bias. All patients in the group had dengue fever, and all methods used in the evaluation and management of the patients were according to the criteria defined by the 2009 World Health Organization (WHO) guidelines. Patients' demographic information, pre-existing diseases, clinical manifestations and laboratory data, were collected by standardized data collection forms. Hematology and biochemistry tests were performed at the Department of Laboratory Medicine of Kaohsiung Medical University Hospital.

Patients who only provided single samples were excluded. During the same periods, we also enrolled patients who had microbiologically confirmed gram-negative bacilli (GNB) and gram-positive cocci (GPC) bacteremia. Patients diagnosed as influenza A virus (Flu A) infection by positive results of their nasopharyngeal swab specimens using Alere BinaxNOW Influenza A&B Card (Alere Scarborough, Maine, USA), were also enrolled for comparison.

Some of the patients suffered from chronic kidney disease stages 3, 4, or 5, i.e. patients who had an estimated glomerular filtration rate (eGFR) of <60 ml/min per 1.73 m^2 at hospital visit [42]. Twenty adult healthy persons, who came to the hospital for their routine health examination, were enrolled as control group.

2.2. Diagnosis of dengue virus infection

All the laboratory diagnostic methods for dengue virus infection were performed at the Center for Disease Control (CDC), Department of Health, Taiwan. Laboratory-confirmed dengue patients meant that the patient had at least one positive result from a NS1 Ag STRIP (Bio-Rad Laboratories, Marnes-la-Coquette, France) or a real-time reverse transcription polymerase chain reaction (real-time RT-PCR) using patients' serum [41–43]. Further serotyping using real-time RT-PCR of nonstructural protein genes were analyzed by detection with serotype-specific primers and probes (Table S2). In brief, the viral RNA was extracted using Viral RNA mini kit (Qiagen, Cat. No. 52906, Chatsworth, CA, USA), treated with RQ1 RNase-free DNase I and reverse transcribed using PrimeScript reagent kit (TaKaRa, Cat. No. RR037A, Kyoto, Japan), according to the manufacturer's instructions. The resulting cDNA was evaluated for dengue viral serotypes by real time RT-PCR (Applied Biosystems, 7500, Foster, USA).

We identified anti-dengue IgG and IgM antibodies in laboratory-confirmed dengue patient's serum. Qualitative measurement of human anti-dengue IgG and IgM antibodies were performed by an ELISA according to the manufacturer's instruction (Abcam, ab108728, and ab108729, Bristol, United Kingdom). Following the WHO 2009 guidelines, primary and secondary dengue infections were distinguished based on the IgG/IgM antibody ratios. Dengue infection was defined as primary if the IgG/IgM ratio was <1.4 (patient's sera at 1/20 dilutions), and secondary if the ratio was >1.4. The laboratory-confirmed cases with samples that were negative in the IgG capture ELISA assay during the febrile phase (within 3 days of illness) were also classified as primary cases, regardless of the IgG/IgM ratio [43].

2.3. Clinical definitions

According to the revised 2009 World Health Organization (WHO) guidelines, dengue infected symptomatic patients can be categorized into three levels of severity: dengue without warning signs (dengue WS-negative), dengue with warning signs (dengue WS-positive) and severe dengue (Fig. S1 a). Dengue patients with warning signs require strict observation and medical intervention.

Patients were evaluated daily within the hospital according to the symptoms of severity as listed in the WHO 2009 guidelines, i.e. [1] abdominal pain or tenderness; [2] persistent vomiting; [3] clinical fluid accumulation; [4] mucosal bleeding; [5] lethargy or restlessness; [6] liver enlargement >2 cm; [7] increase in hematocrit concurrent with rapid decrease in platelet count. For each patient it was determined whether WS developed (≥1 of these 7 symptoms and signs) or not. Clinical fluid accumulations (including pleural effusion and ascites) were confirmed by ultrasound examination. Patients were followed until their recovery or discharge from the hospital (including discharge due to death). If WS developed at any time during the illnesses, the patients were considered to be in the WS-positive group, otherwise, they were considered to be in the WS-negative group. WS-positive patients who never got severe dengue throughout the illnesses were defined as “moderate cases”. In order to compare patients without and with WS and minimize the confounding effects of patient management, we excluded patients who did not visit the hospital to receive treatment within three days after their symptoms onset in the further analysis. This step made sure that patients for further analyses were evaluated, treated, and followed up by the recommendations based on the WHO 2009 guidelines.

2.4. Detection of plasma cytokine and NS1 levels

The plasma levels of several cytokines and growth factors were measured by commercial kits (eBioscience, San Diego, CA, USA), including IL-6 (Cat. No. 88–7066-88), IL-8 (Cat. No. 88–8086-88), IL-10 (Cat. No. 88–7106-88), TNF-α (Cat. No. 88–7346-88), MCP-1 (Cat. No. 88–7399-88), and TGFβ1 (Cat. No. 88–8350-22). In part of patients, the plasma NS1 levels were also measured by using a commercial kit (Arigo Biolaboratories, Nashua, NH, USA, Cat. No. ARG81357).

2.5. Cell culture

Human dermal fibroblast cultures were established from patients, after approval, undergoing breast reduction surgery (Plastic Surgery Department, University Hospital, Uppsala, Sweden), as described [44], and used between passages 6–10. Cells were grown in Dulbecco's modified Eagle's medium (DMEM; Sigma-Aldrich, Cat. No. D5796, St. Louis, MO, USA) containing 10% or 0.5% (under starvation) fetal bovine serum (FBS; Biowest, Biotech-IgG AB, Sweden).

Human telomerase-immortalized microvascular endothelial (TIME) cells were generously provided by Dr. Martin McMahon (University of California, San Fransisco, USA) [45]. The cells were cultured in endothelial growth medium (EBM-2, PromoCell, Cat. No. C-22221, Heidelberg, Germany), supplemented with 5% or 2% (under starvation) fetal calf serum (FCS), 5 ng/ml epidermal growth factor, 0.5 ng/ml vascular endothelial growth factor, 10 ng/ml fibroblast growth factor, 20 ng/ml insulin-like growth factor, 1 μg/ml ascorbic acid and 0.2 μg/ml hydrocortisone, and used between passages 18 and 30. Under proliferative conditions, TIME cells were grown at 37 °C in 5% CO_2 on plastic dishes, and under differentiating conditions cells were grown on Matrigel (13.5 mg/ml; Corning, Cat. No. 356231, Bedford, MA, USA) forming vessel-like structures. Both fibroblasts and endothelial TIME cells were free from mycoplasma contamination.

Human THP-1 monocytes were cultured in RPMI-1640 medium (Sigma-Aldrich, Cat. No. R0883, St. Louis, MO, USA) containing 10% FBS and 2 mM of L-glutamine at 37 °C in 5% CO_2.

2.6. RNA isolation and real time RT-PCR analysis

Total cellular RNA was extracted from dermal fibroblasts and TIME cells (cultured under proliferative or differentiating conditions), using an RNeasy Mini kit (Qiagen, Ref. No. 74106, Hilden, Germany), following the manufacturer's instructions. Differentiating TIME cells were released by digestion of the Matrigel for 45 min, at 37 °C, with 400 μl of 50 U Dispase/ml (BD Biosciences). The enzymatic activity was then inhibited by addition of 800 μl of 10 mM EDTA in PBS. After centrifugation and washings in PBS, RNA or protein (see below) were prepared from the cell lysates. Then, one μg of total RNA was reverse-transcribed to cDNA using the iScript cDNA synthesis kit (Biorad, Cat. No. 1708891, Sweden). Real-time qPCR was carried out on a Biorad bcfx96 cycler using KAPA SYBR Fast (Techtum Lab AB, Sweden) in triplicates (95 °C, 2 min; 40 × (95 °C, 10 s; 60 °C, 30 s)). The primer sequences used for *HAS1*, *HAS2*, *HAS3*, *HYAL1*, *HYAL2*, *CD44*, *TLR4* and *GAPDH*, are listed in Table S2. The expression level of each target gene was normalized to the endogenous reference gene *GAPDH*, and was calculated as $2^{-\Delta CT}$ (ΔCT = CT (sample mRNA) − CT (*GAPDH* mRNA)).

2.7. Quantification of hyaluronan levels in patients´ serum as well as conditioned media of dermal fibroblast and microvascular endothelial cultures

Patient serum samples were processed on the day of collection and stored at −80 °C. Serum hyaluronan levels were measured by an ELISA kit (R&D system, Cat. No. DY3614–05, Minneapolis, MN, USA). Day zero was defined as the day of the onset of the symptoms.

Fibroblasts (100,000 cells/well) or TIME cells (200,000 cells /well) in 6-well plates, were grown in media containing 10% FBS (fibroblasts) or

5% FCS (TIME cells) for 24 h, then starved for an additional 24 h in media supplemented with 0.5% FBS or 2% FCS, respectively. The quiescent cells were then cultured for the indicated time periods in the absence or presence of NS1 protein (recombinant dengue virus serotype 2 non-structural protein 1 derived from strain Thailand/16681/84 and purchased from Enzo, ENZ-PRT105–0100, NY, USA), TGFβ (TGFβ1, Peprotech Nordic, Sweden), TNFα (Peprotech Nordic, Sweden), or combinations thereof. The NS1 protein was reported to be endotoxin-free, by using the Limulus Amebocyte Lysate assay (<0.1 EU/ml in 25 μg of NS1). Conditioned media were collected and the hyaluronan levels were quantified by an enzyme-linked immunosorbent assay, as described before [44]. The specificity of this assay is based on the highly specific and irreversible binding of hyaluronan to immobilized G1 global domain of aggrecan.

2.8. Immunofluorescence staining for hyaluronan and VE-cadherin

Human dermal fibroblasts (5×10^4 cells/well) and proliferating TIME cells (1×10^5 cells/well) were seeded on coverslips in 12-well plates. After 24 h of starvation, untreated or NS1-treated cells were fixed with 3.7% formaldehyde in PBS for 10 min followed by three washes with PBS containing 10% ethanol, and quenching with 100 mM glycine for 30 min. Non-specific binding was then blocked with PBS containing 3% BSA, 5% goat serum (Thermo Fisher, Sweden) and streptavidin plus biotin (Molecular Probes, Cat. No. E-21390, Eugene, Oregon, USA). After washings, cells were incubated over-night with biotinylated-hyaluronan binding protein (b-HABP; 3 μg/ml) [46] and for one hour with a monoclonal antibody against CD44 which does not affect its binding to hyaluronan (Hermes3; 2 μg/ml) [47]. Alexa Fluor 488-Streptavidin conjugate (1:1000; Molecular Probes) and Alexa Fluor 568-labeled goat anti-mouse antibodies (1:1000; Molecular Probes) were used to detect hyaluronan and CD44, respectively. As a specificity control for hyaluronan staining, b-HABP was preincubated for 2 h at 4 °C with 100 μg/ml hyaluronan prior to its addition to the cultures.

To detect VE-cadherin and actin filaments in confluent monolayers of TIME cells grown on Matrigel-coated coverslips (2×10^5 cells/well in 12 well plates), cell cultures were fixed with 4% paraformaldehyde for 15 min and blocked with IgG-free 1% BSA. Cultures were incubated overnight at 4 °C with antibodies against VE-cadherin (4 μg/ml) followed by anti-mouse Alexa-fluor 488 conjugated secondary antibody (1:1000, Invitrogen) for 1 h. Actin was visualized by TRITC-phalloidin (Invitrogen) for 30 min. The nuclei were stained with DAPI and the slides were mounted with ProLong gold antifade reagent (Thermo Fisher, P36930, Eugene, OR, USA). Photographs were taken with a Zeiss Axioplan 2 immunofluorescence microscope (Carl Zeiss AB, Sweden) using Velocity software, and staining was quantified using Image J.

2.9. Binding of THP-1 monocyte-derived macrophage-like cells to fibroblasts or TIME cells

In order to investigate the recruitment of immune cells to dermal fibroblasts and TIME cells, human THP-1 immortalized monocyte-like cells were treated with phorbol 12-myristate 13-acetate (PMA; Sigma-Aldrich, Cat. No. P1585, St. Louis, MO, USA), 5 ng/ml for 48 h, to obtain monocyte-derived macrophage-like cells [48]. Fibroblasts and TIME cells were seeded on the coverslips, and then incubated in media containing 0.5% FBS or 2% FCS, respectively, together with 3 μg/ml NS1, in the absence or presence of a monoclonal CD44 antibody (Hermes1; 50 μg/ml, Bio X Cell, BE0262), which specifically inhibits the binding of hyaluronan to the CD44 receptor. After 24 h, THP-1 monocyte-derived macrophage-like cells, detached by EDTA, were co-cultured with fibroblasts or TIME cells for 20 min. After gentle washing with serum-free RPMI-1640 medium, the coverslips were fixed and stained for hyaluronan and CD44, as described above. Ten randomly taken 20× fields were obtained for each condition and the bound THP-1 cells were counted.

2.10. Western blot analysis

Dermal fibroblasts and TIME cells, growing under proliferative or differentiating conditions, were lysed in ice-cold buffer containing 50 mM Tris-HCl, pH 8.0, 150 mM NaCl, 1% NP-40, 0.1% SDS, 0.5% sodium deoxycholate, supplemented with protease inhibitors (0.5 μg/ml Pefabloc, 10 μM Leupeptin, 9100 KIU/ml Aprotinin) and phosphatase inhibitors (50 mM NaF, 1 mM orthovanadate) and incubated on ice for 30 min, followed by centrifugation at 13,000 rpm at 4 °C for 15 min. TIME cells cultured on Matrigel were subjected to Dispase digestion prior to cell lysis. Protein concentration was measured by utilizing a BCA assay (Thermo Fisher scientific, Gothenburg, Sweden). Samples with equal protein content were subjected to SDS-polyacrylamide gel electrophoresis (SDS-PAGE), followed by wet transfer to nitrocellulose membrane (Amersham, GE Healthcare, Sweden). Membranes were blocked in 5% BSA in Tris buffered saline (TBS) supplemented with 1% Tween 20, and incubated with antibodies (listed in Table S2) at 4 °C overnight. Immunocomplexes were detected by incubation with horseradish peroxide-conjugated secondary goat anti-rabbit IgG (1/10000; Thermo Fisher Scientific, Gothenburg, Sweden, Cat# 65–6120, RRID: AB_2533967) and goat anti-mouse IgG (1/10000; Thermo Fisher Scientific, Gothenburg, Sweden, Cat# 31430, RRID:AB_228307) for 1 h at room temperature, developed by chemiluminescence (Millipore, MA, USA) and protein bands were scanned and quantified by Bio-Rad Universal Hood II CCD camera (Bio-Rad, Hercules, CA, USA).

2.11. Time-lapse microscopy of endothelial tubulogenesis

An in vitro three-dimensional tubulogenesis assay that simulates the final stages of in vivo vessel formation, i.e. cellular differentiation, elongation into tubular structures and lumenogenesis was established, as described [22]. In brief, ice-cold 12-well plates were coated with 200 μl growth factor-reduced Matrigel (13.5 mg/ml; Corning, Cat. No. 356231, Bedford, MA, USA) per well, resulting in an 1 mm thick gel. After Matrigel solidification (at 37 °C for at least 30 min), 4×10^5 TIME cells were seeded on top of the gel-containing plates. The morphogenesis of TIME endothelial cells into tube-like structures appeared after about 6 h and lasted up to 25 h. Time-lapse microscopy (Nikon-Eclipse Ti—U, Japan) was performed on TIME cells differentiated for 16 h before treatment with NS1 or not, followed by time-lapse monitoring for up to 9 h.

2.12. Transwell permeability assay

The permeability of confluent endothelial TIME cell monolayers, treated or not with NS1, was measured by an in vitro transwell permeability assay that mimic human endothelium in vivo [49]. In brief, TIME cells (2×10^5), expressing or depleted of CD44, were grown in a 24-Transwell® (pore size: 0.4 μm; Corning, Kennebunk, ME, USA) for 5 days until a confluent monolayer was formed. Silencing of CD44 was obtained by transient transfection with 20 nM siRNA (ON-TARGET*plus* SMARTpool from Dharmacon, Thermo Fisher Scientific, Sweden) using SilenFECT transfection reagent (Biorad laboratories AB, Sweden) according to the manufacturer's instructions. Fresh starvation media was added in the upper chambers in the absence or presence of exogenously added hyaluronan (25 μg/ml of a molecular mass of 1000 kDa; Q-Med, Sweden) and Hermes1 antibodies (50 μg/ml) overnight. Next, some of the samples were treated for 6 h with NS1 protein (6 μg/ml) with or without *Streptomyces* hyaluronidase (5 units/ml; Sigma-Aldrich, H1136, USA), then media was aspirated, and 200 μl fresh serum-free media containing 3 μl of streptavidin-horseradish peroxidase (HRP) (GE Healthcare, RPN1231, UK) was added. To measure the HRP that leaked through the endothelial monolayer, the inserts were moved to

a new 24-well plate with 500 μl/well of serum-free media and incubated for 5 min at 37 °C. Media from each lower chamber (20 μl), was transferred to a 96-well plate and analyzed for HRP activity by adding 100 μl 3,3′,5,5′-tetramethylbenzidine (TMB) substrate (Sigma-Aldrich, T4444, USA). The color development was detected by an EnSpire Multimode Reader (PerkinElmer, Sweden) at 450 nm.

2.13. Molecular size analysis of hyaluronan in supernatants of TIME cells

Analysis of the size of hyaluronan produced by endothelial microvascular conditioned media, was performed by agarose gel electrophoresis, essentially as described in the online protocol (PEGNAC_HA_Size; NHLBI award number PO1HL107147). Briefly, the supernatants of differentiated TIME cells treated, or not, with NS1 were collected after 25 h and incubated with proteinase K (Ambion, Cat. No. #AM2546) at a final concentration of 0.1 μg/μl at 60 °C for 4 h. Then 4 volumes of pre-chilled (−20 °C) 100% ethanol were added to each sample, followed by incubation overnight at −20 °C. Samples were then centrifuged (4000 rpm for 10 min, room temperature) and the pellets were washed by 1 ml pre-chilled (−20 °C) 75% ethanol. Then the suspensions were centrifuged and the supernatant was removed with a pipette. After the pellets had air-dried for 20 min at room temperature, 200 μl of 100 mM ammonium acetate (Sigma, Cat. No. #A1542) was added to each sample, followed by vortexing and a short spin down. After 20 min incubation at room temperature, proteinase K was heat inactivated at 100 °C for 5 min. Then the samples were chilled on ice for 5 min and nucleic acids were digested by DNase (25 U/μl, overnight at 37 °C). The DNase was then inactivated at 95 °C for 5 min and samples were precipitated again by pre-chilled 100% ethanol (overnight, −20 °C). The samples were then centrifuged, the supernatants discarded, and the pellets washed with 1 ml pre-chilled (−20 °C) 75% ethanol. After another centrifugation at 13,000 rpm for 10 min, the supernatant were discarded, and samples were left to air-dry (20 min). Pellets were re-suspended by adding 100 μl of 100 mM ammonium acetate, then lyophilized on a centrifugal vacuum concentrator, re-suspended in 15 μl of 10 M formamide, and left overnight at 4 °C. Then the samples were loaded on a 2% agarose gel (SeaKem GTG Agarose, made with TAE buffer), and electrophoresed at 100 V (constant voltage) for 50 min. Hyaluronan standards of known sizes were run in parallel (1000 kDa and 480 kDa, Q-Med and Pharmacia, respectively, Uppsala, Sweden; 120 kDa, Hylumed Medical, Genzyme, MA, USA; 30 kDa, Fidia Farmaceutici S.p.A., Italy) [50,51]. The gel was then equilibrated with 30% ethanol for 1 h, and then incubated with Stains-All solution (Sigma, Cat. No. #E9379, final concentration 25 μg/ml), in 30% ethanol in dH_2O. After incubation overnight at room temperature in the dark, the gel staining solution was replaced by dH_2O. After 1 h destaining, the gel was scanned (Epson).

2.14. TCA precipitation of recombinant viral NS1 protein forms in conditioned medium

Conditioned media from dermal fibroblasts treated with NS1 for 24 h, was collected and precipitated by 10% (v/v) trichloroacetic acid on ice for 15 min. The mixture were centrifuged at 4 °C for 10 min and the supernatants discarded. The pellets were re-suspended in 100 μl distilled water and 1 ml chilled 100% acetone was added. After vortexing, samples were left at −20 °C overnight, and then centrifuged. The pellets were then air-dried, lysed in 2× sample buffer, and subjected to SDS-PAGE followed by wet transfer to nitrocellulose membrane and an overnight incubation with NS1 antibodies (dilution 1/500). Immunocomplexes were detected with horseradish peroxide-conjugated secondary antibodies (dilution 1/10000; Invitrogen, Life Technologies Europe BV, Sweden).

2.15. Fluorescein diacetate /propidium iodide staining of live/dead cells

Fluorescein diacetate (FDA) (Sigma-Aldrich, D6883, USA) and propidium iodide (PI) (Sigma-Aldrich, Cat. No. P4170, USA) stainings were performed to detect viable and dead cells, respectively, in fibroblasts and TIME cultures upon treatment with viral NS1 protein. Briefly, untreated cells or cells treated with NS1 (up to 9 μg/ml) for different time periods up to 72 h, were stained in serum-free medium containing 8 μg/ml FDA or 20 μg/ml PI at room temperature for four min, in the dark. After washing by PBS, each sample was analyzed with fluorescence microscopy. Cell viability was measured by counting the FDA-signal (viable green fluorescent cells) and the PI-signal (red nuclei PI-stained dead cells) among 300 cells.

2.16. Statistical analysis

Data were presented as numbers; chi-square test or Fisher's exact test was performed. Univariate and multivariate logistic regression was performed to detect which factors were associated with warning signs. Factors which significantly associated in univariate analysis were included in the multivariate model. The ROC curve was used to examine the predictive value of hyaluronan. The optimal cutoff value of hyaluronan to distinguish patients with warning signs from those without was selected using maximized Youden index, which was defined as [sensitivity+specificity]-1. For examination of the null hypothesis that AUC is equal to 0.5, which indicates no prediction is possible, the Wilcoxon rank sum test was used. Continuous variables from patients were analyzed by Student's *t*-test unless otherwise mentioned. Statistical analyses were performed by IBM SPSS statistical software version 22 for Windows (IBM Corp., Armond, New York, USA). Two-tailed $p < .05$ indicated statistical significance. For in-vitro experimental samples, two-tailed Student's t-test was used to calculate significance. All error bars in the graphics indicate the standard error of the mean (SEM).

3. Results

3.1. Aberrant increase of serum hyaluronan characterizes moderate-to-severe dengue virus infection

A total of 250 patients with laboratory-confirmed dengue virus infection were enrolled during the dengue outbreaks in Taiwan in 2014 to 2015 (Fig. 1 a). Of the enrolled patients, 142 visited the hospital after 3 days of the onset of symptoms (i.e., they did not come to hospital during their febrile phase of illness), whereas 108 patients were examined in both febrile and critical phases of dengue infection.

Because severe dengue infection is associated with vascular dysfunction, and since hyaluronan is a major component of the endothelial glycocalyx and is involved in the regulation of endothelial permeability [52,53], we investigated the levels of hyaluronan in serum of the patients. The 250 dengue infected patients provided consecutive serum samples during the febrile, critical and/or recovery phases. Interestingly, serum hyaluronan levels increased about 100-fold in patients with dengue fever (mean value: 1002 ng/ml) compared to healthy controls ($n = 20$, mean value: 11 ng/ml), as early as 24 h after symptoms onset (Fig. 1 b). The highest concentrations were reached between 4 and 5 days (about 4000 ng/ml) and declined 8 to 10 days after the onset of symptoms, periods corresponding to the critical and recovery phases, respectively. The hyaluronan levels remained elevated during the recovery phase (Fig. 1 b).

A clinical deterioration is seen in severe cases of dengue virus infection, including increased hematocrit and thrombocytopenia, increased vascular permeability and bleedings. The laboratory analyses demonstrated that the increased serum hyaluronan levels (Fig. 1 b) correlated to increased hematocrit (Fig. 1 c) and low platelet counts (Fig. 1 d); the former two increased significantly during day 4–5 and

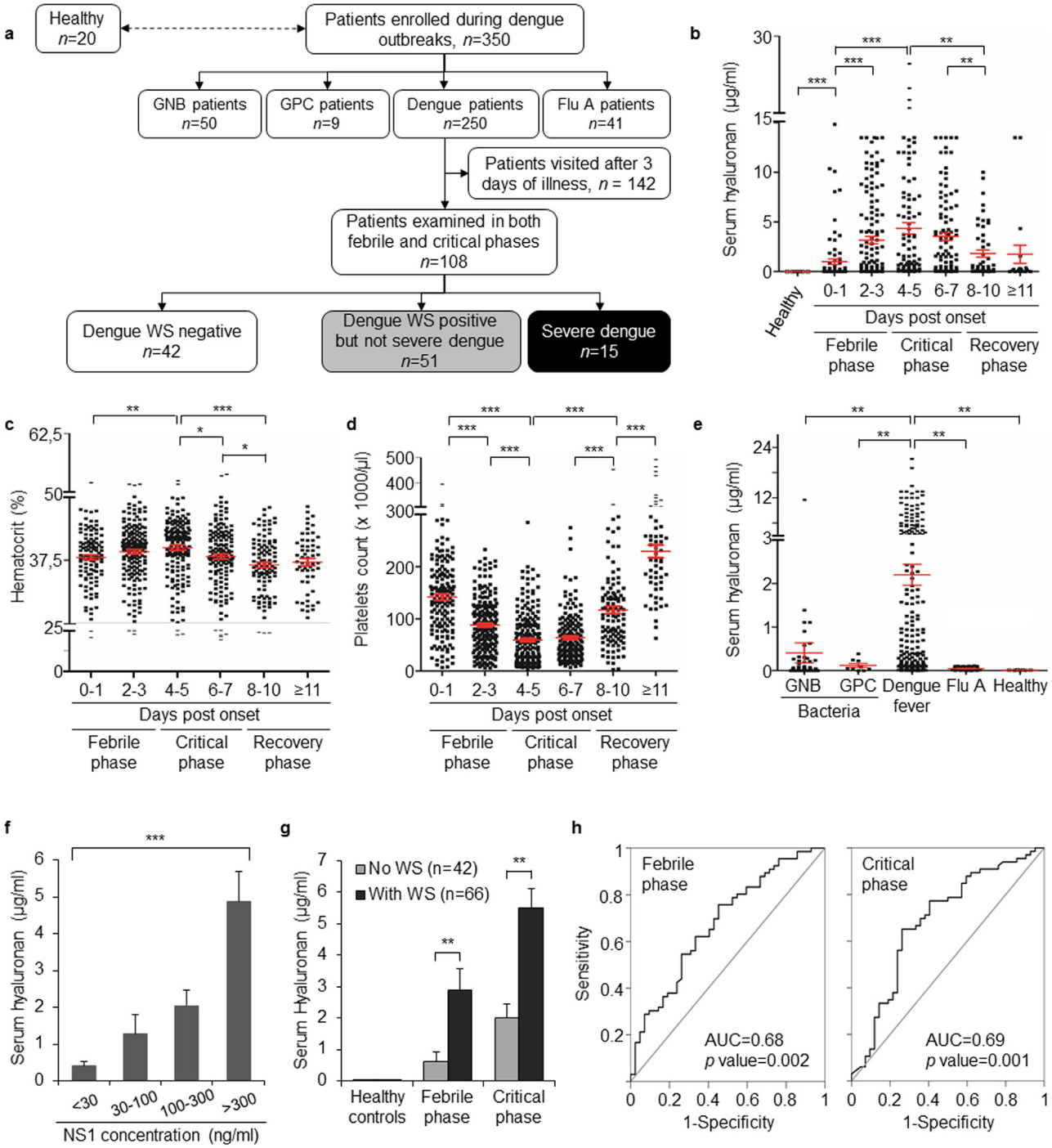

Fig. 1. Serum hyaluronan levels increase robustly in patients with dengue fever and constitute a biomarker for disease severity. (**a**) Flow chart of the enrollment of patients during dengue outbreaks. Twenty healthy adults were enrolled as control group for comparison. Laboratory-confirmed dengue patients, and gram-negative bacilli (GNB), gram-positive cocci (GPC) bacteremia and influenza A virus (Flu A) infected patients were enrolled and analyzed. For further comparison between dengue patients without and with warning signs (WS), patients who did not visit hospital or were not evaluated day by day within 3 days after symptoms onset ($n = 142$) were excluded from the analyses described in panels **g** and **h** below. **(b-d)** Serum hyaluronan levels **(b),** hematocrit **(c)** and platelet counts **(d)** in 250 dengue virus infected patients the days after symptoms onset. **(e)** Serum hyaluronan levels of patients infected with bacteria, dengue virus or influenza virus, as well as of healthy controls. **(f)** Correlation between circulating NS1 concentrations and serum hyaluronan levels in patients with dengue fever ($n = 182$) are depicted. Statistical analysis was carried out by One-way ANOVA (analysis of variance). **(g)** Serum hyaluronan levels from 108 patients who provided paired serum samples during their febrile and critical phases, respectively, exhibiting WS or not. **(h)** ROC (receiver operating characteristic) curve of the serum hyaluronan concentration in febrile and critical phases show that it is a predictor of the occurrence of WS throughout the entire period of illness. Area under curve (AUC) was 0.68 and 0.69 respectively (See also Fig. S1 e). In **(b-g)**, * $p < .05$, ** $p < .01$, *** $p < .001$.

then declined during day 8–10, whereas the platelet counts declined significantly during day 4–5 and then increased during day 8–10.

For comparison, the levels of hyaluronan were also determined in serum of patients infected with other agents, i.e. gram-negative bacilli (GNB; 50 patients), gram-positive cocci (GPC; 9 patients) and influenza A virus (Flu A; 41 patients) on the day of hospital visit. Notably, dengue patients exhibited 5-fold, 10-fold and 40-fold higher hyaluronan levels in comparison to GNB, GPC and Flu A infected patients, respectively (Fig. 1 e). Thus, dengue virus infection triggers an accumulation of hyaluronan, much higher than that induced during infection with influenza virus A or bacteria. Interestingly, high plasma NS1 levels in dengue patients correlated with higher circulating hyaluronan levels (from 182

dengue patients); a 10-fold increase in the circulating viral NS1 protein was accompanied with a 10-fold increased serum hyaluronan levels (Fig. 1 f).

3.2. Increased serum hyaluronan level is an early biomarker for development of warning signs for severe dengue

In an effort to evaluate the importance of hyaluronan as a possible prognostic biomarker for dengue WS positive and severe dengue, the levels of hyaluronan and warning signs were analyzed in the febrile and critical phases of 108 patients (Fig. 1 g, and Table 1). Forty-two patients were evaluated as WS-negative and 66 were WS-positive. In total, 15 patients progressed to severe dengue and all of them had warning signs (Table 1 and Table S1). The means of febrile-phase and critical-phase hyaluronan levels were significantly higher in patients with warning signs compared with those without (Fig. 1 g). Results of univariate and multivariate logistic regression analysis of the demographic data, pre-existing medical condition and laboratory data of the patients, are depicted in Table 1. In univariate analysis among 108 patients, age ≥ 65 years, secondary infection, febrile phase serum hyaluronan level ≥ 70 ng/ml, and critical phase serum hyaluronan level ≥ 2700 ng/ml, were all risk factors for occurrence of warning signs ($p < .01$).

Importantly, after adjustment of age, and secondary dengue virus infection, we still found that febrile phase serum hyaluronan concentration ≥ 70 ng/ml is an independent predictor of occurrence of warning signs (adjusted OR: 2.8, $p = .02$), as is critical phase serum hyaluronan level ≥ 2700 ng/ml (adjusted OR: 4.0, $p < .01$) (Table 1). Thus, serum hyaluronan levels correlate with the severity of the disease.

In addition, the predictive role of serum hyaluronan levels in discriminating dengue WS-negative and WS-positive cases was explored by analysis of the receiver operating characteristic (ROC) curve. The analyses showed significant discriminatory power of serum hyaluronan levels from febrile phase (the area under curve, AUC = 0.68, $p = .002$) and critical phase (AUC = 0.69, $p = .001$) of dengue infection, to distinguish WS-positive from WS-negative patients (Fig. 1 h). Serum hyaluronan levels correlated negatively to platelet counts (Fig. S1 b) and positively to NS1 plasma concentrations (Fig. S1 c). Increased hyaluronan levels are also seen in patients with other diseases, e.g. diabetes. Subdivision of our cohort in patients with ($n = 23$) and without ($n = 85$) diabetes, revealed borderline elevation of hyaluronan levels in both febrile and critical phases (Fig. S1 d). The sensitivity and specificity for febrile phase hyaluronan level were 76% and 55%, respectively, whereas the sensitivity and specificity for critical phase hyaluronan level were 65% and 74%, respectively (Fig. S1 e). Furthermore, we divided the 108 patients into 4 groups according to their febrile phase (early) serum hyaluronan levels (0–25, 25–50, 50–75, 75–100 percentiles ranking, respectively). We found that the percentage of patients with warning signs (left panel), nadir platelet counts <50,000/μl (left middle panel), hematocrit level increasing >20% (middle panel), hypoalbuminemia <30 mg/ml (right middle panel) and occurrence of pleural effusion or ascites (right panel), increased gradually along with the increase of febrile phase serum hyaluronan levels (Fig. S1 f). The latter three symptoms and signs are typical manifestations of plasma leakage in dengue patients. These findings demonstrate that the serum

Table 1
Clinical characteristics and laboratory data of subgroups without or with warning signs, as well as the results of univariate and multivariate logistic regression of the risk factors associated with warning signs.

	Warning signs							
			Univariate		Multivariate			
	Negative	Positive			Febrile phase		Critical phase	
	($n = 42$)	($n = 66$)	OR (95% CI)	p value	Adjusted OR (95% CI)	p value	Adjusted OR (95% CI)	p value
Demographic data								
Sex, male	23	31	0.7 (0.3–1.6)	n.s.				
Age ≥ 65 years	10	34	**3.4 (1.4–8.0)**	**<0.01***	2.0 (0.8–5.2)	n.s.	2.3 (0.9–5.9)	n.s.
Pre-existing medical condition								
Secondary dengue infection	17	43	**2.8 (1.2–6.1)**	**0.01***	2.0 (0.8–4.8)	n.s.	1.2 (0.5–3.2)	n.s.
Bronchial asthma	0	2	not available	n.s.				
Hepatitis B/C virus	3	12	2.9 (0.7–13.9)	n.s.				
Liver cirrhosis	1	0	not available	n.s.				
Hypertension	16	37	2.1 (0.9–4.6)	n.s.				
Diabetes mellitus	7	16	1.6 (0.6–4.3)	n.s.				
Chronic kidney disease	2	10	3.6 (0.7–17.2)	n.s.				
Rheumatoid arthritis	1	0	not available	n.s.				
Laboratory data								
Febrile phase								
DENV 1[a]	9	9	0.6 (0.2–2.1)	n.s.				
DENV 2[a]	22	36	1.8 (0.6–5.9)	n.s.				
DENV 3[a]	1	0	not available	n.s.				
Hyaluronan ≥70 ng/ml	19	50	**3.8 (1.7–8.7)**	**<0.01***	**2.8 (1.2–6.8)**	**0.02***		
WBC < 3000/μl	8	11	0.9 (0.3–2.6)	n.s.				
Platelet <100,000/μl	11	26	1.8 (0.8–4.4)	n.s.				
Albumin <30 mg/ml	2	13	4.9 (0.97–33.5)	n.s.				
AST > 40 IU/L	20	39	1.6 (0.7–3.7)	n.s.				
ALT >40 IU/L	11	28	2.1 (0.8–5.3)	n.s.				
Critical phase								
Hyaluronan ≥2700 ng/ml	11	43	**5.3 (2.2–12.4)**	**<0.01***			**4.0 (1.5–10.3)**	**<0.01***
Hematocrit change >20%	14	33	2.0 (0.8–4.8)	n.s.				

Abbreviations: WBC, white blood cells; AST, aspartate aminotransferase; ALT, alanine aminotransferase; CI, confidence interval; n.s., not significant.
Significant differences are in bold.
[a] Seventy-seven patients (71%) could be identified to be infected by different serotypes of dengue virus.
* $p < .05$, significantly different between warning signs.

hyaluronan level is a useful biomarker to predict the occurrence of warning signs during the entire disease course. Thus, the febrile phase serum hyaluronan level can be used to predict the progress of disease, and thereby determine which dengue patients need hospitalization.

3.3. Exposure to dengue protein NS1 differentially modulates hyaluronan biosynthesis and CD44 expression in dermal fibroblasts and microvascular endothelial cells

To elucidate the molecular mechanisms underlying the excessive accumulation of hyaluronan in serum of dengue-infected individuals, we investigated the effects of recombinant viral NS1 protein; the preparation contained monomeric and oligomeric forms as revealed by immunoblotting (Fig. S2 a). Using fluorescein diacetate / propidium iodide assay, we verified that treatment of dermal fibroblasts and endothelial cells with up to 9 μg NS1/ml did not affect the viability of cells (Fig. S2 b and d). NS1 treatment of dermal fibroblasts potently stimulated the expression of *HAS1*, *HAS2* and *HAS3* (Fig. 2 a). Noteworthy, the basal *HAS2* transcript levels in fibroblast cultures was 100-fold higher than *HAS1* and *HAS3* transcripts, and it was further 3-fold increased at 6 h after NS1 treatment (Fig. S2 c). NS1 did not affect the amount of *HYAL1* and *HYAL2* transcripts, but significantly increased the high basal *CD44* mRNA level in dermal fibroblasts (Fig. 2 a).

NS1 treatment of proliferating TIME cells significantly induced the expressions of *HAS1*, *HAS2* and *HAS3*, as well as *HYAL1*, but had no effect on the intrinsic constitutively high transcription of *HYAL2* and *CD44* (Fig. 2 b). Notably, the induction of *HAS2* transcription was more profound than *HAS1* and *HAS3* after 24 h of exposure to NS1, and was accompanied by increased HAS2 protein expression (Fig. 2 b, Fig. S2, e and f).

The NS1-induced increase in the mRNA levels of the HAS isoforms was accompanied by increased hyaluronan concentrations in the cell culture media of both fibroblasts and endothelial cells (Fig. 2 c). Fibroblasts produced 5–10 times more hyaluronan than endothelial cells. Since the HAS2 isoform dominated, at least in fibroblasts, it is likely that HAS2-synthesized hyaluronan accounted for most of the excessive hyaluronan levels.

3.4. Organization of hyaluronan matrix around human dermal fibroblasts and microvascular endothelial cells

We compared the organization of hyaluronan matrices in dermal fibroblast (Fig. 2 d) and TIME cell (Fig. 2 e) cultures in response to NS1 treatment. Interestingly, in NS1 treated fibroblast cultures, hyaluronan matrices formed a fibrous network spanning multiple cells, in comparison to untreated cultures (Fig. 2 d; each channel is shown separately in Fig. S3 a). Abundant hyaluronan-rich fibrous cables, longer than 20 μm weaving over the cells were predominantly seen in NS1-treated fibroblast cultures, compared to untreated control cells (Fig. S3 b and c, respectively). Hyaluronan-rich fibrous network structures were formed to a much lesser extent around TIME cells compared to fibroblasts (Fig. 2 e; each channel is shown separately in Fig. S3 a); instead the hyaluronan-based matrices in microvascular endothelial cultures exhibited dot-like structures. The specificity for hyaluronan staining was verified by saturation of b-HABP with excess of hyaluronan prior its addition, leading to abrogation of hyaluronan staining (Fig. S3 d).

3.5. Macrophage-like cell adhesion to NS1-induced hyaluronan-rich structures is mediated by CD44

In an effort to understand the increased immune response associated with dengue infection, we investigated how PMA-differentiated THP-1 macrophage-like cells adhered to hyaluronan matrices surrounding dermal fibroblasts (Fig. 2 f) and microvascular endothelial cells (Fig. 2 g). We observed an increase in adhesion of CD44 expressing macrophage-like cells onto hyaluronan cables and hyaluronan-rich dot-like structures around NS1-treated fibroblasts and endothelial cultures, respectively. Blocking of CD44-hyaluronan interactions with Hermes 1 antibodies resulted in about 30% and 70% suppression of macrophage adhesion to NS1-treated dermal fibroblasts and endothelial cells, respectively (Fig. 2 h and i). These findings support the notion that NS1-induced hyaluronan matrices enhance the recruitment of inflammatory cells.

3.6. NS1-induced impairment of vessel-like networks correlates to increased levels of hyaluronan and CD44 suppression

TIME cells grown on Matrigel differentiated to tubular structures within 16 h, forming a network. Because hyaluronidase-dependent hyaluronan fragmentation and CD44 expression [2,22] are involved in the differentiation of microvascular endothelial cells, we investigated the effect of NS1 treatment on expressions of hyaluronan synthases and hyaluronidases, as well as *CD44*, during tubular morphogenesis of TIME cells (Fig. 3 a). CD44 can occur as a standard form as well as several variant forms as a result of differential splicing; however, the TIME cells contain almost exclusively the standard CD44 isoform [21]. Interestingly, the transcriptional activities of *HAS1*, *2*, *3*, and *HYAL1*, as well as the constitutively highly expressed *HYAL2*, were significantly induced after treatment of the vessel-like structures for 9 h with NS1. Importantly, NS1 treatment significantly suppressed the expression of the *CD44* transcripts during endothelial differentiation (Fig. 3 a). In accordance, the protein levels of HAS2 and HYAL2 were markedly increased, whereas that of CD44 was decreased by about 30%, after 9 h of NS1 treatment of the endothelial cell vessel-like structures (Fig. 3 b). Interestingly, exposure of differentiated TIME cell to NS1 resulted in the production of increased levels of fragmented hyaluronan in the conditioned medium (Fig. 3 c).

Monitoring the network formed by differentiated TIME cell cultures treated with NS1 by time-lapse microscopy for up to 9 h, revealed a reversal of the endothelial cell self-assembly into tubular structures in NS1-treated cultures. The rate of the endothelial cell detachment from the vessel-like structures was asynchronous (Fig. 3 d). Movies to show this dynamic process are available (Supplementary Videos S1 and S2). Our observations support the notion that NS1-induced hyaluronan and suppression of CD44 increase the levels of polydisparse hyaluronan and perturbs endothelial cell differentiation.

3.7. Dengue virus-mediated activation of circulating pro-inflammatory cytokines contribute to the increased hyaluronan levels

Examination of immune responses in a cohort of 108 patients, revealed significant increases in the levels of several cytokines already during the early febrile phase, that was significantly further increased during the critical phase (Fig. 4 a). The MCP-1 and IL-6 levels increased initially during the febrile phase and then decreased during the critical phase, whereas the levels of TGFβ, TNFα, IL-8 and IL-10 increased significantly during the febrile phase of dengue infection, and remained high during the critical phase.

Because TGFβ and TNFα are potent stimulators of HAS2-synthesized hyaluronan in several cell types [54,55], we investigated the effects of these mediators on NS1-induced hyaluronan production in fibroblast (Fig. 4 b) and endothelial (Fig. 4 c) cultures. The analysis demonstrated that fibroblasts stimulated with TGFβ or TNFα in combination with NS1 exhibited about 2-fold and 4-fold increases in *HAS2* expression, respectively, compared to cell cultures treated with NS1 only (Fig. 4 b). In TIME cells, TNFα stimulation also significantly increased the NS1-induced *HAS2* expression, however, TGFβ did not (Fig. 4 c). In addition, we investigated the effects of TGFβ and TNFα alone or in combination with NS1 on the expression levels of *CD44* and *TLR4,* encoding a receptor for NS1, in these cultures. Neither TGFβ nor TNFα, alone or in combination with NS1, significantly affected *CD44* mRNA expression, whereas TNFα in combination with

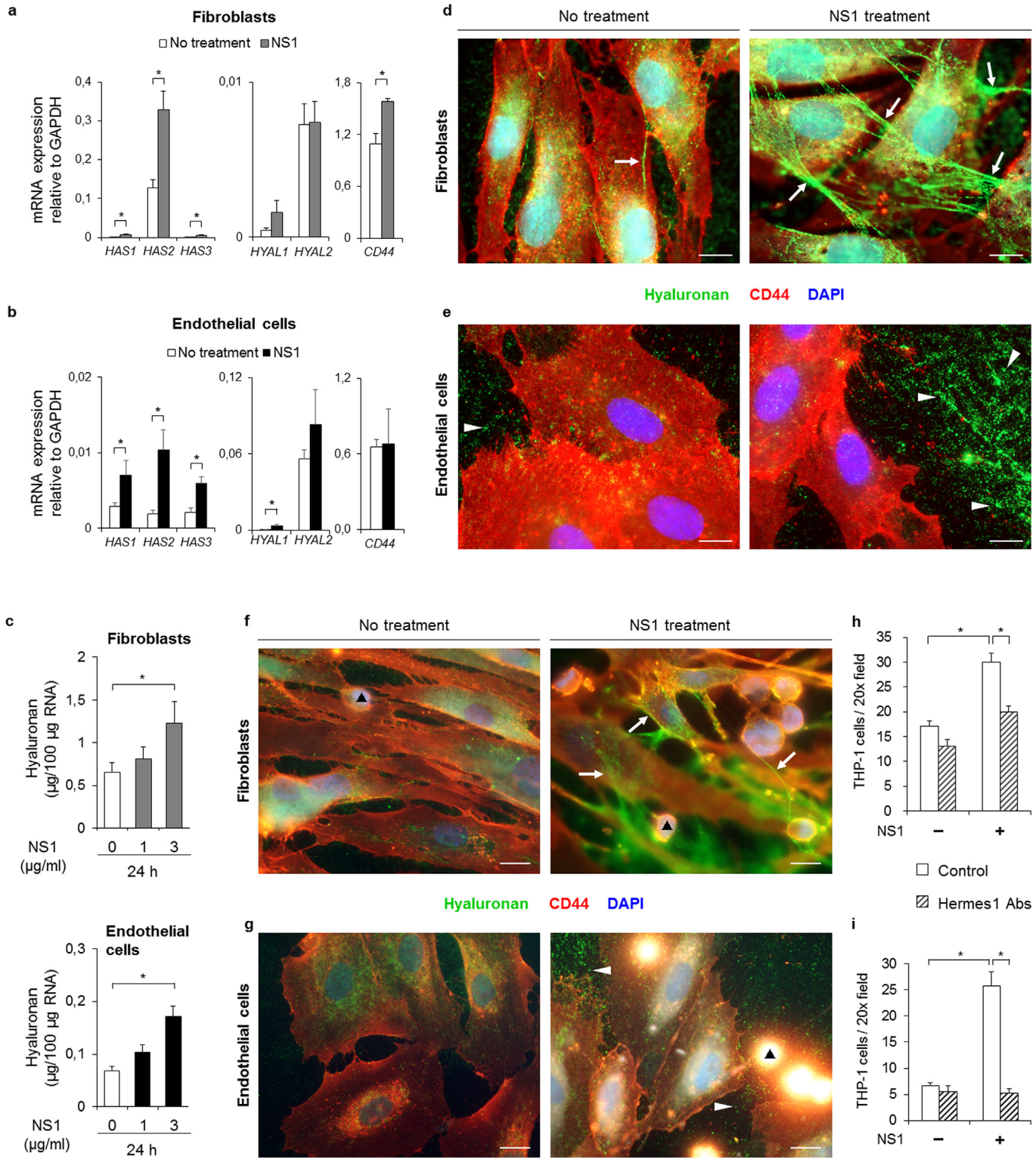

Fig. 2. NS1-treatment of dermal fibroblasts and microvascular endothelial cells enhances synthesis and alters organization of hyaluronan, promoting adhesion of macrophages. **(a-b)** RNA was prepared from human dermal fibroblast **(a)** and proliferative microvascular endothelial **(b)** cultures treated or not with NS1 (3 µg/ml) for 24 h, and reversed transcribed to cDNA; real-time PCR was run using primers for *HAS1,2,3, HYAL1,2* and *CD44* ($n = 3$). **(c)** Analysis of hyaluronan content in conditioned media of fibroblasts (upper panel) and endothelial cells (lower panel) treated or not with NS1 ($n = 3$). **(d-g)** Immunofluorescence of untreated and NS1-treated fibroblasts **(d and f)** and endothelial cells **(e and g)**, exposed to PMA-activated THP-1 human monocyte-derived macrophage-like cells **(f and g)** or not **(d and e)**, were fixed with 3.7% formaldehyde and stained for hyaluronan (green) or CD44 (red); hyaluronan-rich cable-like structures (arrows) and dot-like structures (arrowheads) are depicted. Representative THP-1 cells among several THP-1 cells are marked by black triangles **(f and g)**. See also Fig. S3. **(h and i)** Fibroblasts **(h)** and endothelial cells **(i)** were treated with 3 µg/ml NS1 protein for 24 h, or not, in the absence or presence of Hermes1 (50 µg/ml) antibodies. Then 200,000 PMA-activated THP-1 human monocyte-derived macrophage-like cells (round cells) were co-cultured with fibroblasts and endothelial cells for 20 min, where after non-adherent cells were removed and adherent cells were stained. Ten randomly taken fields (20×) were obtained and the bound THP-1 cells were counted. Quantification of four independent experiments is depicted. In **(a-c)** and **(h-i)**, * $p < .05$. In **(d-g)**, scale bars, 10 µm.

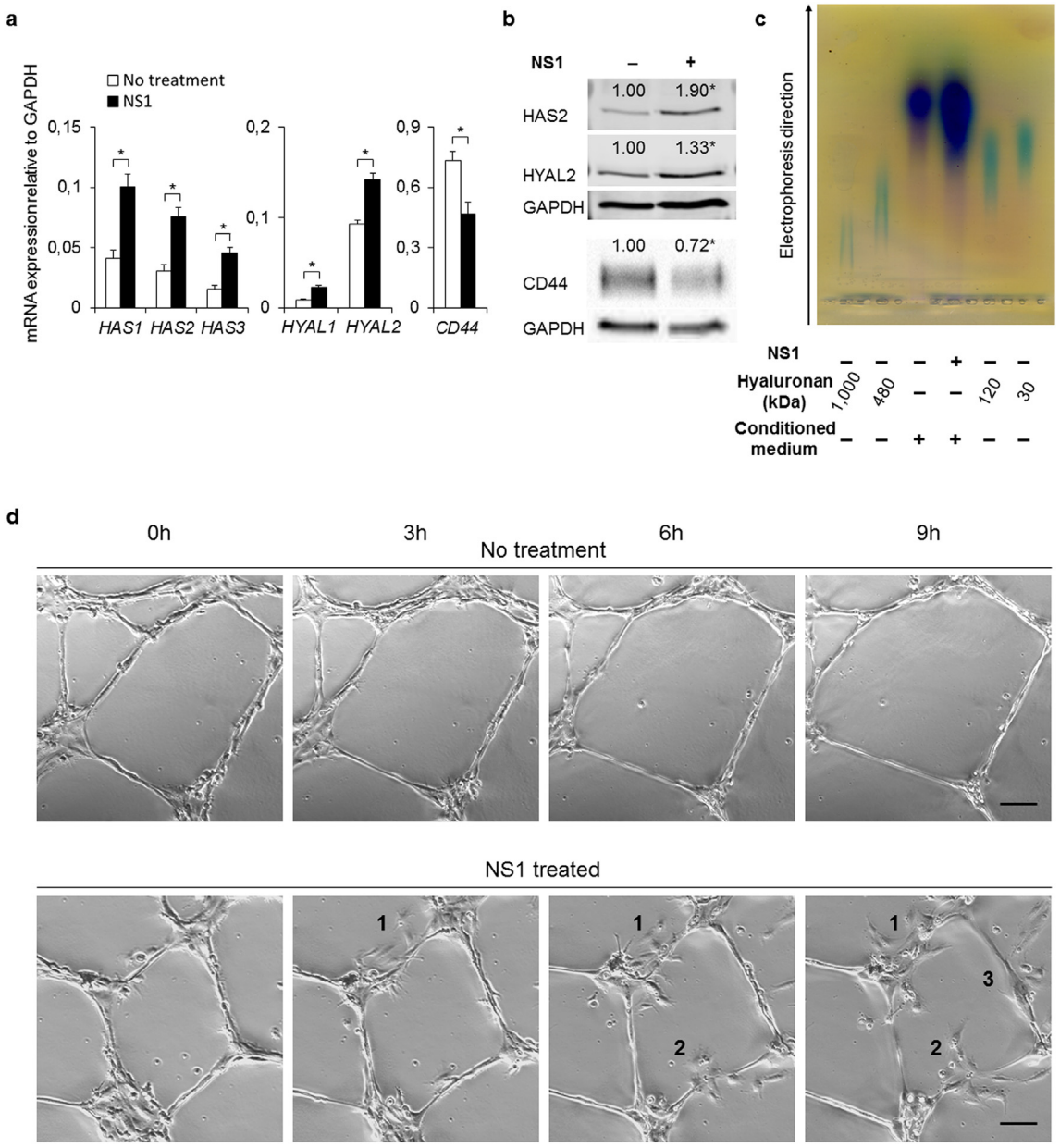

Fig. 3. NS1-treatment of differentiating microvascular endothelial cells results in impaired tubulogenesis. **(a)** Microvascular endothelial TIME cells grown in Matrigel for 16 h, after which cells had differentiated and formed tubular structures, were treated, or not, with 6 μg NS1/ml for an additional 9 h. After harvesting the cells, RNA was prepared and qRT-PCR analyses performed for the expression of mRNAs of *HAS1*, *2*, *3*, *HYAL1*, *2* and *CD44*. The data shown is from three independent experiments performed in triplicates ± SEM. **(b)** Cell lysates of the differentiated tubular endothelial cells were subjected to SDS-PAGE and immunoblotting for HAS2, HYAL2 and CD44, as well as GAPDH as loading control; the densities of the bands were quantified from three independent experiments by ImageJ (depicted by numbers). **(c)** The hyaluronan in 25 h conditioned media from untreated or NS1-treated differentiating endothelial cells, were analyzed for size by agarose electrophoresis, as described in Materials and Methods. **(d)** Microvascular endothelial cells were subjected to NS1 treatment (lower panel) or not (upper panel) during their growth in Matrigel for an additional 9 h after formation of tubular structures. The effect of NS1 on the vessel-like structures are shown. Numbers 1, 2, 3 indicate the order of asynchronous disassembly of vessel-like structures. Scale bars, 100 μm. In **(a-b)**, * $p < .05$.

NS1, synergistically induced the expression of *TLR4* in fibroblast cultures (Fig. 4 b). In microvascular endothelial cultures, NS1 alone markedly induced the expression of *TLR4*, which was partially decreased when NS1 was combined with TGFβ or TNFα. Neither TGFβ nor TNFα, alone or in combination with NS1, significantly affected the transcription of *CD44* in endothelial cells (Fig. 4 c). The hyaluronan levels increased significantly in both fibroblasts and endothelial cell cultures treated with TGFβ and TNFα in combination with NS1.

Thus, circulating cytokines induced during dengue virus infection further enhanced the hyaluronan production induced by NS1.

3.8. Signaling pathways involved in NS1-induced hyaluronan production

To gain insights into the signaling pathways evoked by NS1 which can mediate increased hyaluronan production and signaling, we investigated the activation status of key signaling molecules in fibroblast (Fig. 4 d) and endothelial (Fig. 4 e) cultures. Whereas NS1-treatment of fibroblasts did not affect the NF-B signaling pathway, in endothelial cultures an increase in NF-kB activation was observed within 15 min of NS1 treatment that lasted, with a slight decrease, for up to 4 h (Fig. 4 e). Other signaling pathways, including Akt, and Erk1/2 and p38 MAP-kinases, were activated within 15 min after NS1-treatment,

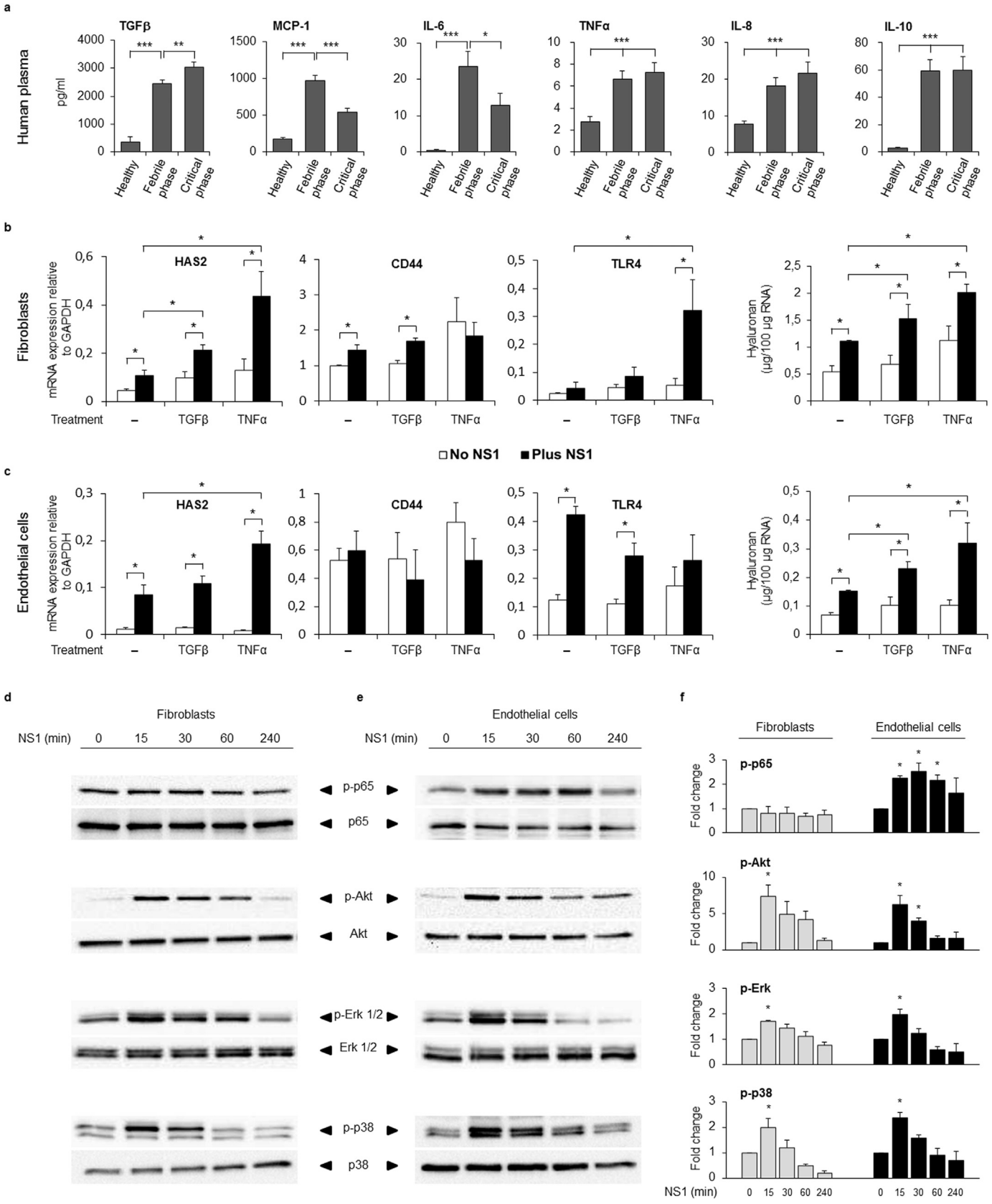

Fig. 4. Dengue virus-induced pro-inflammatory cytokines synergize with NS1 to promote hyaluronan synthesis involving several signaling pathways. **(a)** The levels of TGFβ, MCP-1, IL-6, TNFα, IL-8 and IL-10 were analyzed in 108 dengue patients both in febrile and critical phases, and compared to twenty healthy individuals. **(b-c)** Dermal fibroblasts **(b)** and microvascular endothelial cells grown under proliferative conditions **(c)** were treated (filled bars), or not (open bars), with NS1 (3 μg/ml) alone or in combination with TGFβ (1 ng/ml) or TNFα (10 ng/ml) for 24 h. The expression levels of mRNAs for *HAS2, CD44* and *TLR4* were determined by RT-PCR. The levels of hyaluronan in 24 h conditioned media were also determined (right panels) ($n = 3$, triplicate determinations of each independent experiment). **(d-e)** Dermal fibroblasts **(d)** and endothelial cells **(e)** were treated with NS1 (3 μg/ml) for the indicated time periods. Cell lysates were prepared and proteins were separated by SDS-PAGE and immunoblotted for the phosphorylated and total amount of p65 NF-B, Akt, Erk1/2 and p38 MAP-kinase. **(f)** Quantification of three independent experiments of dermal fibroblasts and endothelial cells are depicted in gray and black bars respectively. * $p < .05$ when compared to the non-treated controls. In **(a-c)** and **(f)**, results are means ± SEM. * $p < .05$, ** $p < .01$, *** $p < .001$.

followed by a similar attenuation pattern, both in fibroblasts and endothelial cultures (Fig. 4, d-f). Thus, NS1 induces several signaling pathways in both cell types.

3.9. Hyaluronan-CD44 interactions regulate NS1-mediated endothelial hyper-permeability

Recently, we demonstrated a critical role of the hyaluronan - CD44 axis in normal vessel formation [22]. Therefore, we investigated the effect of CD44 and hyaluronan on the integrity of untreated and NS1-treated confluent endothelial cell monolayers, using an in vitro endothelium permeability assay. Confluent monolayers not exposed to NS1 exhibited a basal permeability, which was increased by about 3-fold when hyaluronan was added to the culture media or when cells were depleted of CD44 (Fig. 5 a). Treatment with NS1 increased the permeability by about 2-fold compared to non-treated cells. Importantly, hyaluronan stimulation, or silencing of CD44, further enhanced the NS1-induced endothelial permeability (Fig. 5 a). Interestingly, if confluent endothelial cell monolayers were pre-treated by Hermes 1 antibody, which specifically blocks the binding of hyaluronan to CD44, before NS1-treatment, or if the cells were treated with *Streptomyces* hyaluronidase together with NS1, the endothelial hyper-permeability was prevented (Fig. 5 a). These observations suggest a key regulatory role of hyaluronan-engaged CD44 in NS1-induced vascular hyper-permeability.

The NS1-induced endothelial permeability (Fig. 5 a) was accompanied by an increase in the number and size of paracellular gaps, as monitored by immunofluorescence staining (Fig. 5, b and c). In response to stimulation with hyaluronan or knockdown of CD44, morphological changes occurred leading to formation of paracellular gaps, and enlargement of NS1-induced gaps, which was reverted by Hermes1 antibodies or treatment with *Streptomyces* hyaluronidase (Fig. 5 b, c).

CD44-mediated regulation of vascular function occurs partly through modulation of VE-cadherin in adherens junctions [56,57]. As shown in Fig. 6, under basal conditions VE-cadherin was distributed in a striped or jagged fashion delineating confluent and resting endothelial cells, and colocalized with F-actin. There was no significant change in the total VE-cadherin protein expression levels in NS1-treated cells, with or without combination with hyaluronan or Hermes1 pre-treatment, compared to non-treated endothelial cells, neither did depletion of CD44 affect its expression (Fig. S4), suggesting that hyaluronan/CD44 does not affect VE-cadherin expression. Importantly, stimulation with NS1 or hyaluronan, or CD44 depletion, caused re-distribution and fragility of VE-cadherin (Fig. 6). Immunofluorescence analysis of TRITC-phalloidin-stained endothelial cells revealed that hyaluronan stimulation induced both longer (Fig. S5 a) and thicker (Fig. S5 b) F-actin stress fibers compared to control cells; CD44 depletion also promoted the formation of longer and thicker F-actin stress fibers (Fig. 6 and Fig. S5). Notably, a co-localization of VE-cadherin with the ends of F-actin stress fibers at sites of cell-cell junctions, was observed. Our observations support the notion that NS1, or treatment with hyaluronan or CD44 suppression, affects VE-cadherin and cytoskeletal associations, modulating endothelial-endothelial intercellular junctions (Fig. 6).

4. Discussion

We demonstrate that NS1-mediated increase in circulating hyaluronan predicts the occurrence of warning signs during dengue virus infection, and promotes endothelial hyper-permeability involving perturbed CD44-hyaluronan interactions accompanied by F-actin stress fibers and VE-cadherin re-organization. The circulating levels of dengue virus NS1 protein in patients with dengue virus infection range between 0.02 and 15 μg/ml [58,59]. Circulating NS1 is thought to play key regulatory roles in the pathology of dengue virus infection, but insights into the pathogenesis of severe vascular leakage have been hampered by the lack of an animal model that accurately mimics the transient capillary permeability syndrome seen in patients [37,39,60]. Previous studies have reported increased serum hyaluronan levels and a potential association to dengue severity, but the increased levels of hyaluronan was detected at later infection phases and the underlying molecular mechanisms were not elucidated [43,53,61]. We have confirmed and extended these findings, by studying a larger and early-enrolled cohort of dengue virus infected patients. We provide evidence that hyaluronan levels higher than 70 ng/ml during early infection, is an independent predictor for occurrence of warning signs and thus severe dengue fever. Importantly, we show that high circulating NS1 levels, indicative of disease severity, correlate with high concentration of serum hyaluronan (Fig. 1, Table 1 and Table S1).

Patients with severe dengue sometimes show life-threatening increase in vascular permeability. Important regulators of vascular permeability are endothelial tight junctions and adherence junctions. In particular, homophilic interactions of VE-cadherin molecules between endothelial cells regulate the intercellular junctions by undergoing actin-controlled movement along intercellular contacts [62,63]. Our findings show that NS1 treatment did not affect the amount of VE-cadherin in endothelial cells, however, its localization was rearranged, which was accompanied by a rearrangement of actin filaments resulting in increased gaps between endothelial cells (Figs. 5 and 6). Stimulation with hyaluronan or knockdown of CD44 resulted in similar morphological alterations, suggesting that the effect of NS1 on rearrangement of VE-cadherin and actin filaments is, at least partially, mediated by perturbed hyaluronan-CD44 interactions.

Hyaluronan-dependent pericellular matrices have been shown to surround cells in culture [11,64]. During the inflammatory phase after a virus infection, cells synthesize and secrete hyaluronan that form inflammatory cable-like hyaluronan-rich structures [65]. Analysis of the effects of the dengue NS1 protein on dermal fibroblasts and endothelial cell cultures revealed that the expression of genes involved in the biosynthesis and signaling of hyaluronan was modulated. Fibroblasts produced 5–10 times higher levels of hyaluronan compared to endothelial cells (Fig. 2 c), however, given that during viremia and presence of large amounts of NS1, endothelial cells in the entire circulation may be exposed to NS1, their contribution to the elevated hyaluronan levels in dengue patients may be substantial. Importantly, NS1 exposure resulted in the deposition of different forms of hyaluronan-rich matrices in fibroblasts and endothelial cultures, and both structures attracted immune cells (Fig. 2). Indeed, the size of hyaluronan macromolecular structures play a pivotal role not only for the physical, but also for the immunological properties of tissues. Whereas alveolar macrophages constitutively bind, take up and degrade hyaluronan [66–68], the capacity of monocytes to bind hyaluronan is induced in response to pro-inflammatory cytokines during inflammation or infection [69]. Our observations that depletion of CD44 or treatment with excessive amounts of hyaluronan leads to enhanced endothelial hyper-permeability suggests that the size and signaling of hyaluronan matrices have an important role in the regulation of vessel function.

Our previous studies on the differentiation of TIME cells demonstrated that CD44 was predominantly localized at the fusion sites during tubulogenesis, and that knock-down of CD44 or HYAL2 resulted in an inability of endothelial cells to differentiate and form tubular structures [22]. The inability of CD44-depleted microvascular endothelial cells to form vessel-like structures, together with our previous studies that hyaluronan fragments trigger CD44-mediated tubulogenesis in a CXCL1-dependent manner [2], suggest key regulatory roles for hyaluronan-engaged CD44 and chemokines in angiogenesis. In addition to degrade hyaluronan, HYAL2 has been reported to regulate the formation of the glycocalyx via CD44-ERM-related cytoskeletal interactions [70], to serve as a viral entry receptor [71] and to regulate CD44 alternative splicing events affecting cell phenotype in progressive fibrosis [72]. The NS1-mediated induction of hyaluronan synthesizing and

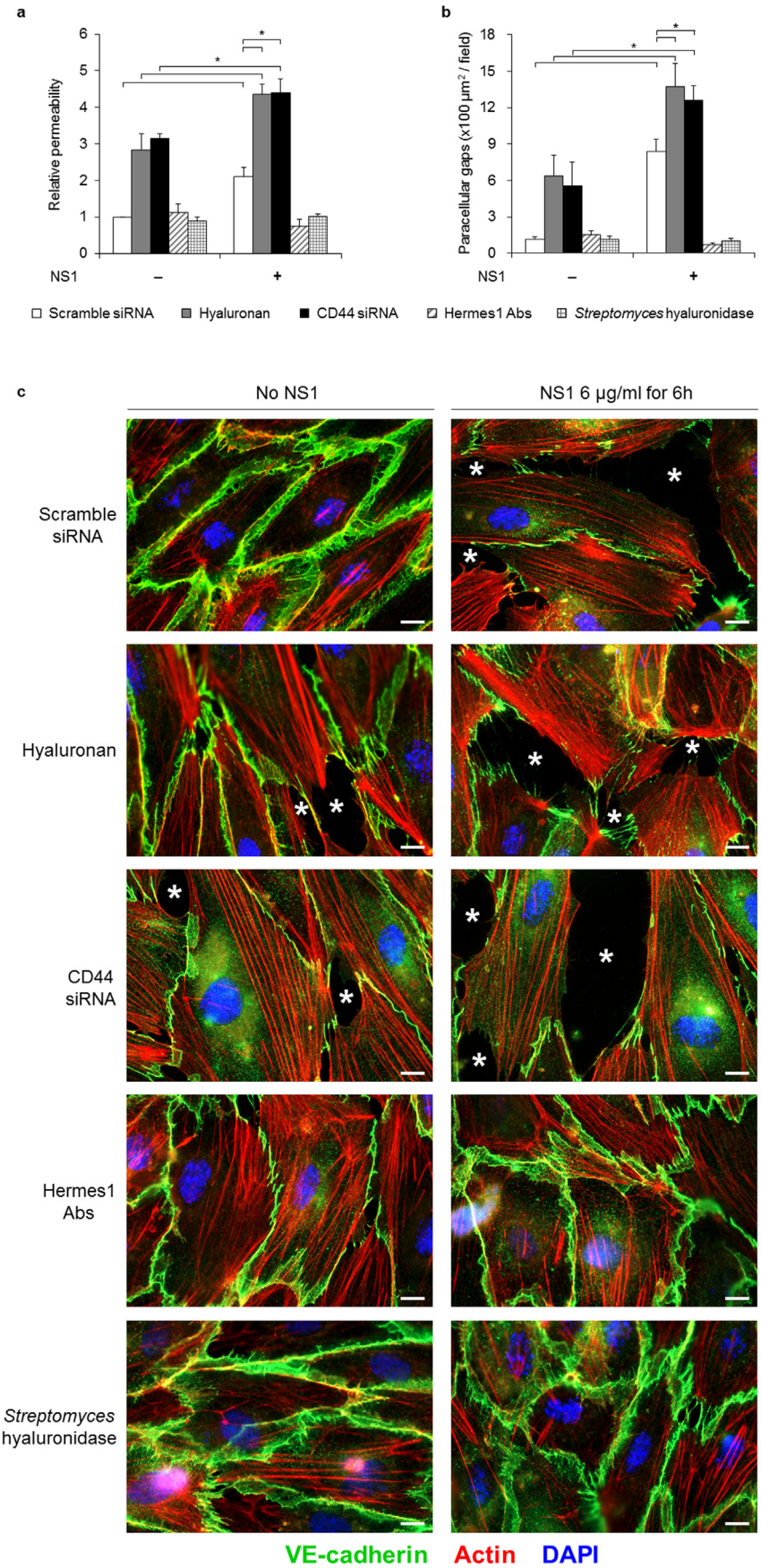

Fig. 5. Hyaluronan-CD44 interactions are important for the stability of intercellular adhesion junctions. **(a)** Confluent monolayers of microvascular endothelial cells expressing or depleted of CD44, were pre-treated or not with exogenous hyaluronan (25 µg/ml) or Hermes1 antibodies (50 µg/ml) overnight. Then, cell monolayers were co-treated or not with 6 µg/ml NS1 protein and some cultures also with *Streptomyces* hyaluronidase (5 units/ml) for 6 h. The permeability was determined by using an in vitro transwell permeability assay (n = 3). **(b-c)** Confluent microvascular endothelial cells, expressing or depleted of CD44, grown on Matrigel-coated coverslips, were treated as described in **(a),** fixed and stained for VE-cadherin

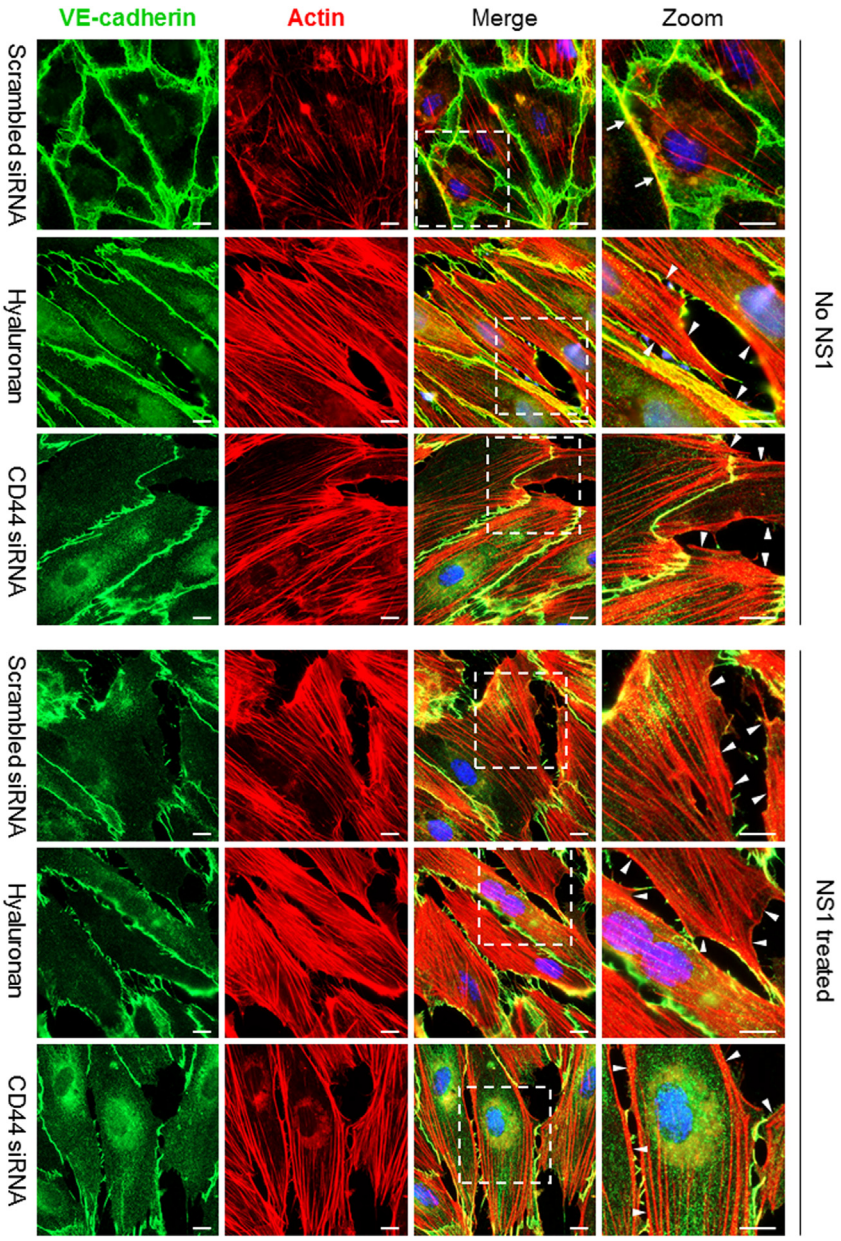

Fig. 6. Effect of NS1, CD44 depletion and hyaluronan on VE-cadherin localization. Human microvascular endothelial TIME cells (2×10^5 cells/well in 12-well plates), transfected with CD44 siRNA or control, scrambled siRNA, were stimulated with 25 g/ml hyaluronan overnight, fixed in 4% paraformaldehyde and stained for VE-cadherin (green) and actin filaments (TRITC-phalloidin; red). Photographs were taken with a Zeiss Axioplan 2 immunofluorescence microscope. Arrows indicate the co-localization of VE-cadherin with actin fibers. Arrowheads indicate the discontinuity and fragility of VE-cadherin. Scale bars, 10 μm.

catabolizing enzymes (Figs. 2, 3), resulting in the formation of proinflammatory fragmented hyaluronan-rich matrices, and may have contributed to disorganization of the glycocalyx layer [27]. Intriguingly, the hyaluronidase TMEM2 (homolog to KIAA1199) [73] was recently shown to have a pivotal role in normal angiogenesis during embryonic development, by balancing hyaluronan depolymerization [74]. Furthermore, the accumulated knowledge about the role of HYAL1 and HYAL2 in glycocalyx function support the notion that hyaluronan is important for endothelial cell function [75,76].

Previous studies have demonstrated key regulatory roles of cytokines released by monocytes/macrophages, T cells and endothelial cells, in the pathogenesis of dengue virus infection [33,77]. The release of soluble mediators and cytokines, such as TGFβ, MCP-1, IL-6, MMPs and TNFα, predispose endothelial cells to apoptosis and endothelial damage [31,78]. Our observations that cytokines increase in the circulation during the various phases of dengue virus illness (Fig. 4), and that TGFβ and TNFα promote NS1-induced biosynthesis of hyaluronan in dermal fibroblasts and microvascular endothelial cells (Fig. 4, b and c), emphasize their importance during dengue infection. Since fragmented hyaluronan functions as a proinflammatory danger-associated molecular pattern (DAMP) affecting TLR signaling [79,80], NS1-mediated induction of HASs and HYALs drives the release of both fragmented hyaluronan and pro-inflammatory cytokines promoting inflammation. Our data demonstrated activation of Akt, p38, and Erk1/2 in both fibroblasts and endothelial cells, as well as of NF-B in endothelial cells, in response to NS1; however, the precise signaling pathways activated by NS1 that induces hyaluronan synthesis, remain to be elucidated.

Through interaction with TLR4 on monocytes, NS1 has been shown to trigger the release of proinflammatory cytokines promoting vascular leakage during dengue infection [32,35–38]. In addition, NS1-induced plasma leakage is associated with perturbation of endothelial glycocalyx

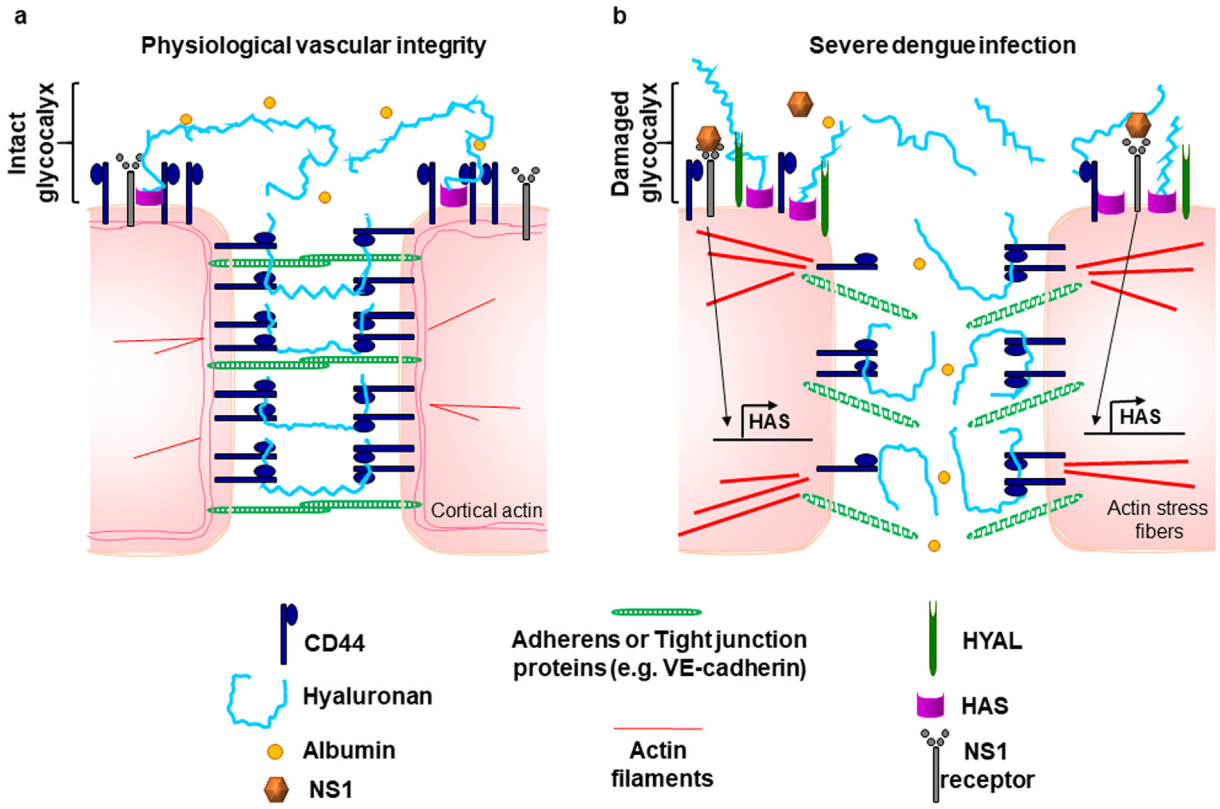

Fig. 7. Schematic illustration of a possible mechanism for NS1-induced increased endothelium permeability. **(a)** Under physiological conditions, balanced expression of CD44 and hyaluronan levels contribute to cell-to-cell adhesion by cross-bridging between cells and maintaince of an intact glycocalyx. **(b)** During severe dengue virus infection, the excessive levels of partly fragmented hyaluronan occupy the reduced number of CD44 receptors, thus preventing efficient cross-bridging. In addition, disruption of the glycocalyx layer may contribute to increased permeability. It should be noted that in cells in which CD44 had been knocked down, NS1 still enhanced the disruption of junctional proteins, such as VE-cadherin (Figs. 5 and 6), suggesting that perturbed hyaluronan-CD44 interactions is not the only mechanism involved in NS1-induced vascular leakage.

and intercellular junctions, including adherens junctions [32,53]. In a recent study, NS1-induced vascular leakage was shown to be independent of inflammatory cytokines but dependent on endothelial glycocalyx layer components, such as sialic acid and heparan sulfate proteoglycans [37,39]. Both in vitro and in vivo studies have demonstrated that NS1 protein via TLR4 disrupts endothelial barrier function triggering vascular leakage [32,81]. NS1 has been shown to promote the destruction of adherens and tight junctions [53]. The expression of CD44 promotes the assembly of junctional proteins and its abrogation leads to reduction of VE-cadherin leading to opening of intercellular gaps [56]. Our observation that the NS1-induced decreased expression of CD44 is connected with an increased endothelial permeability (Fig. 5), is consistent with this notion. We also observed that exogenously added hyaluronan potentiated NS1-mediated endothelial cell permeability, suggesting that excessive levels of hyaluronan causes occupation of CD44 expressed by the endothelium, and thus perturb normal hyaluronan-CD44 interactions, as schematically depicted in Fig. 7.

There are 4 different serotypes of dengue virus epidemics globally. In our cohort, most of the patients were infected by the type 2 serotype, and the recombinant NS1 protein we used for in vitro study was also obtained from this viral strain. Further analyses of patients infected by the different serotypes, the effect of the different NS1 proteins, and the involvement of increased levels of hyaluronan, are ongoing.

In conclusion, our data show that the dengue NS1 protein and pro-inflammatory factors stimulate hyaluronan biosynthesis and alters hyaluronan-CD44 interactions leading to disorganization of intercellular junctions and vascular leakage. Discerning the molecular mechanisms underlying the increased vascular permeability will help to formulate a strategy to prevent plasma leakage during dengue infection.

Supplementary data to this article can be found online at https://doi.org/10.1016/j.ebiom.2019.09.014.

Author contributions

Study conception and design of research studies: PH, YHC, CYL. Provision of patient samples and interpretation of data: CYL, YHC, CHHu. Design and performance of experiments, acquisition and analysis of data: CYL, PH, CK, CHHe. Writing and editing of manuscript: PH, CYL, CHHe, YHC, CK, CHHu, JT. PH and YHC are the guarantor of completeness of the entire study.

All authors have read and approved the final version of the manuscript.

Declaration of Competing Interest

CYL, YHC and PH have submitted a patent application based on the findings in this manuscript in United states (US 15/881,350) and EU (EP 18155997.2). CYL, YHC and PH are the inventors but not owner of a patent proved in Taiwan (TW I651535). The other authors have declared that no conflict of interest exists.

References

[1] Lennon FE, Singleton PA. Hyaluronan regulation of vascular integrity. Am J Cardiovasc Dis 2011;1(3):200–13.
[2] Takahashi Y, Li L, Kamiryo M, Asteriou T, Moustakas A, Yamashita H, et al. Hyaluronan fragments induce endothelial cell differentiation in a CD44- and CXCL1/GRO1-dependent manner. J Biol Chem 2005;280(25):24195–204.
[3] West DC, Hampson IN, Arnold F, Kumar S. Angiogenesis induced by degradation products of hyaluronic acid. Science 1985;228:1324–6.
[4] Laurent TC, Hyaluronan Fraser JRE. FASEB J 1992;6:2397–404.
[5] Heldin P, Lin CY, Kolliopoulos C, Chen YH, Skandalis SS. Regulation of hyaluronan biosynthesis and clinical impact of excessive hyaluronan production. Matrix Biol 2019;78-79:100–17.
[6] Nagy N, Kuipers HF, Marshall PL, Wang E, Kaber G, Bollyky PL. Hyaluronan in immune dysregulation and autoimmune diseases. Matrix Biol 2019;78-79:292–313.

[7] Petrey AC, de la Motte CA. Hyaluronan, a crucial regulator of inflammation. Front Immunol 2014;5:101.
[8] Lee-Sayer SSM, Dong YF, Arif AA, Olsson M, Brown KL, Johnson P. The where, when, how, and why of hyaluronan binding by immune cells. Front Immunol 2015;6.
[9] Heldin P, Basu K, Kozlova I, Porsch H. HAS2 and CD44 in breast tumorigenesis. Adv Cancer Res 2014;123:211–29.
[10] Turley EA, Wood DK, McCarthy JB. Carcinoma cell Hyaluronan as a "portable" cancerized prometastatic microenvironment. Cancer Res 2016;76(9):2507–12.
[11] Heldin P, Pertoft H. Synthesis and assembly of the hyaluronan-containing coats around normal human mesothelial cells. Exp Cell Res 1993;208:422–9.
[12] Heldin P, Basu K, Olofsson B, Porsch H, Kozlova I, Kahata K. Deregulation of hyaluronan synthesis, degradation and binding promotes breast cancer. J Biochem 2013;154(5):395–408.
[13] Fraser JR, Laurent TC, Laurent UB. Hyaluronan: its nature, distribution, functions and turnover. J Intern Med 1997;242(1):27–33.
[14] Knudson W, Chow G, Knudson CB. CD44-mediated uptake and degradation of hyaluronan. Matrix Biol 2002;21(1):15–23.
[15] Laurent TC, Laurent UBG, Fraser JRE. Serum hyaluronan as a disease marker. Ann Med 1996;28(3):241–53.
[16] Jackson DG, Prevo R, Clasper S, Banerji S. LYVE-1, the lymphatic system and tumor lymphangiogenesis. Trends Immunol 2001;22(6):317–21.
[17] Sallisalmi M, Tenhunen J, Kultti A, Tammi M, Pettila V. Plasma hyaluronan and hemorheology in patients with septic shock: a clinical and experimental study. Clin Hemorheol Microcirc 2014;56(2):133–44.
[18] Weinbaum S, Tarbell JM, Damiano ER. The structure and function of the endothelial glycocalyx layer. Annu Rev Biomed Eng 2007;9:121–67.
[19] Kolarova H, Ambruzova B, Sindlerova LS, Klinke A, Kubala L. Modulation of endothelial glycocalyx structure under inflammatory conditions. Mediators Inflamm 2014;2014:694312.
[20] Sussmann M, Sarbia M, Meyer-Kirchrath J, Nusing RM, Schror K, Fischer JW. Induction of hyaluronic acid synthase 2 (HAS2) in human vascular smooth muscle cells by vasodilatory prostaglandins. Circ Res 2004;94(5):592–600.
[21] Homann S, Grandoch M, Kiene LS, Podsvyadek Y, Feldmann K, Rabausch B, et al. Hyaluronan synthase 3 promotes plaque inflammation and atheroprogression. Matrix Biol 2018;66:67–80.
[22] Olofsson B, Porsch H, Heldin P. Knock-down of CD44 regulates endothelial cell differentiation via NFkappaB-mediated chemokine production. PLoS One 2014;9(3):e90921.
[23] Rahmanian M, Heldin P. Testicular hyaluronidase induces tubular structures of endothelial cells grown in three-dimensional collagen gel through a CD44-mediated mechanism. Int J Cancer 2002;97(5):601–7.
[24] West DC, Kumar S. Hyaluronan and angiogenesis. In: Evered D, Whelan J, editors. The biology of hyaluronan. Ciba Found. Symp. Chichester: Wiley; 1989. p. 187–201.
[25] Medina CO, Nagy N, Bollyky PL. Extracellular matrix and the maintenance and loss of peripheral immune tolerance in autoimmune insulitis. Curr Opin Immunol 2018;55:22–30.
[26] Kuipers HF, Rieck M, Gurevich I, Nagy N, Butte MJ, Negrin RS, et al. Hyaluronan synthesis is necessary for autoreactive T-cell trafficking, activation, and Th1 polarization. Proc Natl Acad Sci U S A 2016;113(5):1339–44.
[27] Ushiyama A, Kataoka H, Iijima T. Glycocalyx and its involvement in clinical pathophysiologies. J Intensive Care 2016;4.
[28] Dogne S, Flamion B, Caron N. Endothelial glycocalyx as a shield against diabetic vascular complications: involvement of hyaluronan and hyaluronidases. Arterioscler Thromb Vasc Biol 2018;38(7):1427–39.
[29] Dejana E, Orsenigo F, Lampugnani MG. The role of adherens junctions and VE-cadherin in the control of vascular permeability. J Cell Sci 2008;121(Pt 13):2115–22.
[30] Dvorak AM, MacGlashan Jr DW, Morgan ES, Lichtenstein LM. Vesicular transport of histamine in stimulated human basophils. Blood 1996;88(11):4090–101.
[31] Guzman MG, Harris E. Dengue. Lancet 2015;385(9966):453–65.
[32] Modhiran N, Watterson D, Muller DA, Panetta AK, Sester DP, Liu LD, et al. Dengue virus NS1 protein activates cells via toll-like receptor 4 and disrupts endothelial cell monolayer integrity. Sci Transl Med 2015;7(304).
[33] Simon-Loriere E, Duong V, Tawfik A, Ung S, Ly S, Casademont I, et al. Increased adaptive immune responses and proper feedback regulation protect against clinical dengue. Sci Transl Med 2017;9(405).
[34] Srikiatkhachorn A. Plasma leakage in dengue haemorrhagic fever. Thromb Haemost 2009;102(6):1042–9.
[35] Chen HR, Chuang YC, Lin YS, Liu HS, Liu CC, Perng GC, et al. Dengue virus nonstructural protein 1 induces vascular leakage through macrophage migration inhibitory factor and autophagy. Plos Neglect Trop D 2016;10(7):e0004828.
[36] Puerta-Guardo H, Glasner DR, Harris E. Dengue virus NS1 disrupts the endothelial Glycocalyx, leading to hyperpermeability. PLoS Pathog 2016;12(7):e1005738.
[37] Glasner DR, Ratnasiri K, Puerta-Guardo H, Espinosa DA, Beatty PR, Harris E. Dengue virus NS1 cytokine-independent vascular leak is dependent on endothelial glycocalyx components. PLoS Pathog 2017;13(11).
[38] Balazs EA, Darzynskiewicz Z, Kulonen E, Pikkarainen J. The effect of hyaluronic acid on fibroblasts, mononuclear phagocytes and lymphocytes. New York: Academic Press; 1973; 237–52.
[39] Puerta-Guardo H, Glasner DR, Espinosa DA, Biering SB, Patana M, Ratnasiri K, et al. Flavivirus NS1 triggers tissue-specific vascular endothelial dysfunction reflecting disease tropism. Cell Rep 2019;26(6):1598–613.
[40] Wang SF, Chang K, Lu RW, Wang WH, Chen YH, Chen M, et al. Large dengue virus type 1 outbreak in Taiwan. Emerg Microbes Infec 2015;4.
[41] Wang SF, Chang K, Loh E, Wang WH, Tseng SP, Lu PL, et al. Consecutive large dengue outbreaks in Taiwan in 2014-2015. Emerg Microbes Infec 2016;5.
[42] Chang K, Huang CH, Lee IK, Lu PL, Lin CY, Chen TC, et al. Differences in mortality and clinical manifestations of dengue Hemorrhagic fever in Taiwan in different years: a comparison for cases in 2014 and 2015 epidemics. American JTropical Med Hygiene 2017;97(2):361–8.
[43] Tang TH, Alonso S, Ng LF, Thein TL, Pang VJ, Leo YS, et al. Increased serum hyaluronic acid and Heparan Sulfate in dengue fever: association with plasma leakage and disease severity. Sci Rep 2017;7:46191.
[44] Li L, Asteriou T, Bernert B, Heldin CH, Heldin P. Growth factor regulation of hyaluronan synthesis and degradation in human dermal fibroblasts: importance of hyaluronan for the mitogenic response of PDGF-BB. Biochem J 2007;404(2):327–36.
[45] Venetsanakos E, Mirza A, Fanton C, Romanov SR, Tlsty T, McMahon M. Induction of tubulogenesis in telomerase-immortalized human microvascular endothelial cells by glioblastoma cells. Exp Cell Res 2002;273(1):21–33.
[46] Jacobson A, Rahmanian M, Rubin K, Heldin P. Expression of hyaluronan synthase 2 or hyaluronidase 1 differentially affect the growth rate of transplantable colon carcinoma cell tumors. Int J Cancer 2002;102:212–9.
[47] Jalkanen S, Bargatze RF, de los Toyos J, ECs Butcher. Lymphocyte recognition of high endothelium: antibodies to distinct epitopes of an 85-95 kDa glycoprotein antigen differentially inhibit lymphocyte binding to lymph node, mucosal, or synovial endothelial cells. J Cell Biol 1987;105:983–90.
[48] Park EK, Jung HS, Yang HI, Yoo MC, Kim C, Kim KS. Optimized THP-1 differentiation is required for the detection of responses to weak stimuli. Inflamm Res 2007;56(1):45–50.
[49] Bischoff I, Hornburger MC, Mayer BA, Beyerle A, Wegener J, Furst R. Pitfalls in assessing microvascular endothelial barrier function: impedance-based devices versus the classic macromolecular tracer assay. Sci Rep-Uk 2016;6.
[50] Kubo K, Nakamura T, Takagaki K, Yoshida Y, Endo M. Depolymerization of hyaluronan by sonication. Glycoconj J 1993;10(6):435–9.
[51] Tavianatou A, Piperigkou Z, Barbera C, Beninatto R, Masola V, Caon I, et al. Molecular size-dependent specificity of hyaluronan on functional properties,morphology and matrix composition of mammary cancer cells. Matrix Biol 2019;3:1–24.
[52] Rahbar E, Cardenas JC, Baimukanova G, Usadi B, Bruhn R, Pati S, et al. Endothelial glycocalyx shedding and vascular permeability in severely injured trauma patients. J Transl Med 2015;13:117.
[53] Suwarto S, Sasmono RT, Sinto R, Ibrahim E, Suryamin M. Association of endothelial glycocalyx and tight and adherens junctions with severity of plasma leakage in dengue infection. J Infect Dis 2017;215(6):992–9.
[54] Porsch H, Bernert B, Mehic M, Theocharis AD, Heldin CH, Heldin P. Efficient TGFbeta-induced epithelial-mesenchymal transition depends on hyaluronan synthase HAS2. Oncogene 2013;32(37):4355–65.
[55] Vigetti D, Genasetti A, Karousou E, Viola M, Moretto P, Clerici M, et al. Proinflammatory cytokines induce hyaluronan synthesis and monocyte adhesion in human endothelial cells through hyaluronan synthase 2 (HAS2) and the nuclear factor-kappaB (NF-kappaB) pathway. J Biol Chem 2010;285(32):24639–45.
[56] Tsuneki M, Madri JA. CD44 regulation of endothelial cell proliferation and apoptosis via modulation of CD31 and VE-cadherin expression. J Biol Chem 2014;289(9):5357–70.
[57] Cerutti C, Ridley AJ. Endothelial cell-cell adhesion and signaling. Exp Cell Res 2017;358(1):31–8.
[58] Allonso D, Meneses MDF, Fernandes CA, Ferreira DF, Mohana-Borges R. Assessing positivity and circulating levels of NS1 in samples from a 2012 dengue outbreak in Rio de Janeiro, Brazil. Plos One 2014;9(11).
[59] Liu Y, Liu JY, Cheng G. Vaccines and immunization strategies for dengue prevention. Emerg Microbes Infec 2016;5.
[60] Simmons CP, Farrar JJ, Nguyen v V, Wills B. Dengue. N Engl J Med 2012;366(15):1423–32.
[61] Honsawek S, Kongtawelert P, Pothacharoen P, Khongphatthanayothin A, Chongsrisawat V, Poovorawan Y. Increased levels of serum hyaluronan in patients with dengue infection. J Infect 2007;54(3):225–9.
[62] Cavey M, Rauzi M, Lenne PF, Lecuit T. A two-tiered mechanism for stabilization and immobilization of E-cadherin. Nature 2008;453(7196):751–U2.
[63] Dejana E, Tournier-Lasserve E, Weinstein BM. The control of vascular integrity by endothelial cell junctions: molecular basis and pathological implications. Dev Cell 2009;16(2):209–21.
[64] Clarris BJ, Fraser JRE, Rodda SJ. Effect of cell-bound hyaluronic acid on infectivity of Newcastle disease virus for human synovial cells *in vitro*. Ann Rheum Dis 1974;33:240–2.
[65] de la Motte CA, Hascall VC, Drazba J, Bandyopadhyay SK, Strong SA. Mononuclear leukocytes bind to specific hyaluronan structures on colon mucosal smooth muscle cells treated with polyinosinic acid:polycytidylic acid inter-alpha-trypsin inhibitor is crucial to structure and function. Am J Pathol 2003;163(1):121–33.
[66] Culty M, Nguyen HA, Underhill CB. The hyaluronan receptor (CD44) participates in the uptake and degradation of hyaluronan. J Cell Biol 1992;116:1055–62.
[67] Teder P, Heldin P. Mechanism of impaired local hyaluronan turnover in bleomycin-induced lung injury in rat. Am J Respir Cell Mol Biol 1997;17:376–85.
[68] Teder P, Vandivier RW, Jiang D, Liang J, Cohn L, Pure E, et al. Resolution of lung inflammation by CD44. Science 2002;296(5565):155–8.
[69] Levesque MC, Haynes BF. Cytokine induction of the ability of human monocyte CD44 to bind hyaluronan is mediated primarily by TNF-alpha and is inhibited by IL-4 and IL-13. J Immunol 1997;159(12):6184–94.
[70] Duterme C, Mertens-Strijthagen J, Tammi M, Flamion B. Two novel functions of hyaluronidase-2 (Hyal2) are formation of the glycocalyx and control of CD44-ERM interactions. J Biol Chem 2009;284(48):33495–508.
[71] Liu SL, Duh FM, Lerman MI, Miller AD. Role of virus receptor Hyal2 in oncogenic transformation of rodent fibroblasts by sheep betaretrovirus Env proteins. J Virol 2003;77(5):2850–8.

[72] Midgley AC, Oltean S, Hascall V, Woods EL, Steadman R, Phillips AO, et al. Nuclear hyaluronidase 2 drives alternative splicing of CD44 pre-mRNA to determine profibrotic or antifibrotic cell phenotype. Sci Signal 2017;10(506).
[73] Yoshida H, Nagaoka A, Kusaka-Kikushima A, Tobiishi M, Kawabata K, Sayo T, et al. KIAA1199, a deafness gene of unknown function, is a new hyaluronan binding protein involved in hyaluronan depolymerization. Proc Natl Acad Sci U S A 2013;110(14):5612–7.
[74] De Angelis JE, Lagendijk AK, Chen HJ, Tromp A, Bower NI, Tunny KA, et al. Tmem2 regulates embryonic Vegf signaling by controlling hyaluronic acid turnover. Dev Cell 2017;40(2):123–36.
[75] Dogne S, Rath G, Jouret F, Caron N, Dessy C, Flamion B. Hyaluronidase 1 deficiency preserves endothelial function and Glycocalyx integrity in early Streptozotocin-induced diabetes. Diabetes 2016;65(9):2742–53.
[76] Kong XQ, Chena L, Yea P, Wang ZM, Zhang JJ, Ye F, et al. The role of HYAL2 in LSS-induced glycocalyx impairment and the PKA-mediated decrease in eNOS-Ser-633 phosphorylation and nitric oxide production. Mol Biol Cell 2016;27(25):3972–9.
[77] Pandey N, Jain A, Garg RK, Kumar R, Agrawal OP, Lakshmana Rao PV. Serum levels of IL-8, IFNgamma, IL-10, and TGF beta and their gene expression levels in severe and non-severe cases of dengue virus infection. Arch Virol 2015;160(6):1463–75.
[78] Chen HC, Hofman FM, Kung JT, Lin YD, Wu-Hsieh BA. Both virus and tumor necrosis factor alpha are critical for endothelium damage in a mouse model of dengue virus-induced hemorrhage. J Virol 2007;81(11):5518–26.
[79] Jiang DH, Liang JR, Noble PW. Hyaluronan as an immune regulator in human diseases. Physiol Rev 2011;91(1):221–64.
[80] Ruppert SM, Hawn TR, Arrigoni A, Wight TN, Bollyky PL. Tissue integrity signals communicated by high-molecular weight hyaluronan and the resolution of inflammation. Immunol Res 2014;58(2–3):186–92.
[81] Beatty PR, Puerta-Guardo H, Killingbeck SS, Glasner DR, Hopkins K, Harris E. Dengue virus NS1 triggers endothelial permeability and vascular leak that is prevented by NS1 vaccination. Sci Transl Med 2015;7(304).